
Don't be so Monotone: Relaxing Stochastic Line Search in Over-Parameterized Models

Leonardo Galli, Holger Rauhut
RWTH Aachen University
Aachen
{galli, rauhut}@mathc.rwth-aachen.de

Mark Schmidt
University of British Columbia
Canada CIFAR AI Chair (Amii)
schmidtm@cs.ubc.ca

Abstract

Recent works have shown that line search methods can speed up Stochastic Gradient Descent (SGD) and Adam in modern over-parameterized settings. However, existing line searches may take steps that are smaller than necessary since they require a monotone decrease of the (mini-)batch objective function. We explore nonmonotone line search methods to relax this condition and possibly accept larger step sizes. Despite the lack of a monotonic decrease, we prove the same fast rates of convergence as in the monotone case. Our experiments show that nonmonotone methods improve the speed of convergence and generalization properties of SGD/Adam even beyond the previous monotone line searches. We propose a POLYak NONmonotone Stochastic (PoNoS) method, obtained by combining a nonmonotone line search with a Polyak initial step size. Furthermore, we develop a new resetting technique that in the majority of the iterations reduces the amount of backtracks to zero while still maintaining a large initial step size. To the best of our knowledge, a first runtime comparison shows that the epoch-wise advantage of line-search-based methods gets reflected in the overall computational time.

1 Introduction

Stochastic Gradient Descent (SGD) [Robbins and Monro, 1951] is the workhorse for the whole Deep Learning (DL) activity today. Even though its simplicity and low memory requirements seem crucial for dealing with these huge models, the success of SGD is strongly connected to the choice of the learning rate. In the field of deterministic optimization [Nocedal and Wright, 2006], this problem is addressed [Armijo, 1966] by employing a line search technique to select the step size. Following this approach, a recent branch of research has started to re-introduce the use of line search techniques for training DL models [Mahsereci and Hennig, 2017, Paquette and Scheinberg, 2018, Bollapragada et al., 2018, Truong and Nguyen, 2018, Vaswani et al., 2019]. These methods have been shown to speed up SGD [Vaswani et al., 2019] and Adam [Duchi et al., 2011, Vaswani et al., 2020] in the over-parameterized regime. However, the existing stochastic line searches may take step sizes that are smaller than necessary since they require a monotone decrease in the (mini-)batch objective function. In particular, the highly non-linear non-convex landscapes of DL training losses suggest that it may be too restrictive to impose such a condition [Grippo et al., 1986]. In addition, the stochastic nature of SGD discourages imposing a monotone requirement on a function that is not directly the one we are minimizing [Ferris and Lucidi, 1994] (mini- vs full-batch function). Furthermore, the recent research on the edge of stability phenomenon [Cohen et al., 2021, Nacson et al., 2022] shows that the best performance for training DL models with Gradient Descent (GD) is obtained when large step sizes yield a nonmonotone decrease of the loss function. In this paper, we propose the use of nonmonotone line search methods [Grippo et al., 1986, Zhang and Hager, 2004] to possibly accept increases in the objective function and thus larger step sizes.

In parallel with line search techniques, many other methods [Baydin et al., 2017, Luo et al., 2019, Mutschler and Zell, 2020, Truong and Nguyen, 2021] have been recently developed to automatically

select the step size. In Asi and Duchi [2019], Berrada et al. [2020], Loizou et al. [2021], Gower et al. [2021, 2022], Li et al. [2022], the Polyak step size from Polyak [1969] has been adapted to SGD and successfully employed to train DL models. However, in this setting, the Polyak step size may become very large and it may lead to divergence or, in more favorable cases, induce the (mini-batch) function to decrease nonmonotonically. Starting from Berrada et al. [2020], the Polyak step size has been upper-bounded to avoid divergence and “smoothed” to prevent large fluctuations [Loizou et al., 2021]. However, this “smoothing” technique is a heuristic and, as we will clarify below, may reduce the Polyak step more than necessary. In this paper, we instead combine the Polyak initial step from Loizou et al. [2021] with a nonmonotone line search. In fact, nonmonotone methods are well suited for accepting as often as possible a promising (nonmonotone) step size, while still controlling its growth. In the deterministic setting, the same optimization recipe has been used in the seminal papers Raydan [1997] (for the Barzilai and Borwein [1988] (BB) step size) and Grippo et al. [1986] (for the unitary step in the case of Newton).

In the over-parameterized regime, the number of free parameters dominates the number of training samples. This provides modern DL models with the ability of exactly fitting the training data. In practice, over-parameterized models are able to reduce to zero the full-batch loss and consequently also all the individual losses. This is mathematically captured by the interpolation assumption, which allows SGD with non-diminishing step sizes to achieve GD-like convergence rates [Vaswani et al., 2019]. We develop the first rates of convergence for stochastic nonmonotone line search methods under interpolation. In the non-convex case, we prove a linear rate of convergence under the Polyak-Lojasiewicz (PL) condition. In fact in Liu et al. [2022], it has been shown that wide neural networks satisfy a local version of the PL condition, making this assumption more realistic for DL models than the Strong Growth Condition (SGC) [Schmidt and Le Roux, 2013].

When considering line search methods for training DL models one has to take into account that they require one additional forward step for each backtrack (internal iteration) and each mini-batch iteration requires an unknown amount (usually within 5) of backtracks. A single forward step may require up to one-third the runtime of SGD (see Section E.6 of the Appendix), thus, too many of them may become a computational burden. Le Roux et al. [2012] proposed a “resetting” technique that is able to (almost) always reduce the number of backtracking steps to zero by shrinking the initial step size [Vaswani et al., 2019]. In this paper, we will show that this technique may have a negative impact on the speed of convergence, even when only employed as a safeguard (as in the “smoothing” technique [Loizou et al., 2021]). As a third contribution, we develop a new resetting technique for the Polyak step size that reduces (almost) always the number of backtracks to zero, while still maintaining a large initial step size. To conclude, we will compare the runtime of different algorithms to show that line search methods equipped with our new technique outperform non-line-search-based algorithms.

2 Related Works

The first nonmonotone technique was proposed by Grippo et al. [1986] to globalize the Newton method without enforcing a monotonic decrease of the objective function. After that, nonmonotone techniques have been employed to speed up various optimization methods by relaxing this monotone requirement. A few notable examples are the spectral gradient in Raydan [1997], the spectral projected gradient in Birgin et al. [2000], sequential quadratic programming methods in Zhou and Tits [1993], and the Polak-Ribière-Polyak conjugate gradient in Zhou [2013].

In the pre-deep-learning era [Plagianakos et al., 2002], shallow neural networks have been trained by combining the nonmonotone method [Grippo et al., 1986] with GD. In the context of speech recognition [Keskar and Saon, 2015], one fully-connected neural network has been trained with a combination of a single-pass full-batch nonmonotone line search [Grippo et al., 1986] and SGD. The Fast Inertial Relaxation Engine (FIRE) algorithm is combined with the nonmonotone method [Zhang and Hager, 2004] in Wang et al. [2019, 2021] for solving sparse optimization methods and training logistic regression models, while a manually adapted learning rate is employed to train DL models. In Krejić and Krklec Jerinkić [2015, 2019], Bellavia et al. [2021], the nonmonotone line search by Li and Fukushima [1999] is used together with SGD to solve classical optimization problems. In concurrent work [Hafshejani et al., 2023], the nonmonotone line search by Grippo et al. [1986] has been adapted to SGD for training small-scale kernel models. This line search maintains a nonmonotone window W (usually 10) of weights in memory and it computes the current mini-batch function value on all of them at every iteration. The method proposed in Hafshejani et al. [2023] is

computationally very expensive and impractical to train modern deep learning models due to the need to store previous weights. In this paper, we instead propose the first stochastic adaptation of the nonmonotone line search method by Zhang and Hager [2004]. Thanks to this line search, no computational overhead is introduced in computing the nonmonotone term which is in fact a linear combination of the previously computed mini-batch function values. To the best of our knowledge, we propose the first stochastic nonmonotone line search method to train modern convolutional neural networks and transformers [Vaswani et al., 2017].

Our paper is the first to combine a line search technique with the Stochastic Polyak Step size (SPS) [Loizou et al., 2021]. In fact, the existing line search methods [Vaswani et al., 2019, Paquette and Scheinberg, 2018, Mahsereci and Hennig, 2017] do not address the problem of the selection of a suitable initial step size. In Vaswani et al. [2019], the authors focus on reducing the amount of backtracks and propose a “resetting” technique (3) that ends up also selecting the initial step size. In this paper, we consider these two problems separately and tackle them with two different solutions: a Polyak initial step size and a new resetting technique (5) to reduce the amount of backtracks. Regarding the latter, a similar scheme was presented in Grapiglia and Sachs [2021], however we modify it to be combined with an independent initial step size (e.g., Polyak). This modification allows the original initial step size not to be altered by the resetting technique.

In this paper, we extend Vaswani et al. [2019] by modifying the monotone line search proposed there with a nonmonotone line search. Our theoretical results extend the theorems presented in Vaswani et al. [2019] to the case of stochastic nonmonotone line search methods. Previous results in a similar context were given by Krejić and Krklec Jerinkić [2015, 2019], Bellavia et al. [2021] that assumed 1) the difference between the nonmonotone and monotone terms to be geometrically converging to 0 and 2) the batch-size to be geometrically increasing. In this paper, we replace both hypotheses with a weaker assumption (i.e., interpolation) [Meng et al., 2020] and we actually prove that the nonmonotone and monotone terms converge to the same value. In Hafshejani et al. [2023], related convergence theorems are proved under the interpolation assumption for the use of a different nonmonotone line search (i.e., Grippo et al. [1986] instead of Zhang and Hager [2004]). However in Hafshejani et al. [2023], no explanation is given on how to use an asymptotic result (Lemma 4) for achieving their non-asymptotic convergence rates (Theorem 1 and 2). Addressing this problem represents one of the main challenges of adapting the existing nonmonotone theory [Grippo et al., 1986, Dai, 2002, Zhang and Hager, 2004] to the stochastic case.

In Vaswani et al. [2019], the rates provided in the non-convex case are developed under an SGC, while we here assume the more realistic PL condition [Liu et al., 2022]. In fact in Liu et al. [2022], not only wide networks are proven to satisfy PL but also networks with skip connections (e.g., ResNet [He et al., 2016], DenseNet [Huang et al., 2017]). For this result, we extend Theorem 3.6 of Loizou et al. [2021] for stochastic nonmonotone line search methods by exploiting our proof technique. In Loizou et al. [2021], various rates are developed for SGD with a Polyak step size and it is possible to prove that they hold also for PoNoS. In fact, the step size yielded by PoNoS is by construction less or equal than Polyak’s. However, the rates presented in this paper are more general since they are developed for nonmonotone line search methods and do not assume the use of any specific initial step size (e.g., they hold in combination with a BB step size).

3 Methods

Training machine learning models (e.g., neural networks) entails solving the finite sum problem $\min_{w \in \mathbb{R}^n} f(w) = \frac{1}{M} \sum_{i=1}^M f_i(w)$, where w is the parameter vector and f_i corresponds to a single instance of the M points in the training set. We assume that f is lower-bounded by some value f^* , that f is L -smooth and that it either satisfies the PL condition, convexity or strong-convexity. Vanilla SGD can be described by the step $w_{k+1} = w_k - \eta \nabla f_{i_k}(w_k)$, where $i_k \in \{1, \dots, M\}$ is one instance randomly sampled at iteration k , $\nabla f_{i_k}(w_k)$ is the gradient computed only w.r.t. the i_k -th instance and $\eta > 0$ is the step size. The mini-batch version of this method modifies i_k to be a randomly selected subset of instances, i.e., $i_k \subset \{1, \dots, M\}$, with $\nabla f_{i_k}(w_k)$ being the averaged gradient on this subset and $|i_k| = b$ the mini-batch size. Through the whole paper we assume that each stochastic function f_{i_k} and gradient $\nabla f_{i_k}(w)$ evaluations are unbiased, i.e., $\mathbb{E}_{i_k}[f_{i_k}(w)] = f(w)$ and $\mathbb{E}_{i_k}[\nabla f_{i_k}(w)] = \nabla f(w)$, $\forall w \in \mathbb{R}^n$. Note that \mathbb{E}_{i_k} represents the conditional expectation w.r.t. w_k , i.e., $\mathbb{E}_{i_k}[\cdot] = \mathbb{E}[\cdot | w_k]$. In other words, \mathbb{E}_{i_k} is the expectation computed w.r.t. ν_k , that is the

random variable associated with the selection of the sample (or subset) at iteration k (see Bottou et al. [2018] for more details).

We interpret the over-parameterized setting in which we operate to imply the interpolation property, i.e., let $w^* \in \operatorname{argmin}_{w \in \mathbb{R}^n} f(w)$, then $w^* \in \operatorname{argmin}_{w \in \mathbb{R}^n} f_i(w) \forall 1 \leq i \leq M$. This property is crucial

for the convergence results of SGD-based methods because it can be combined either with the Lipschitz smoothness of f_{i_k} or with a line search condition to achieve the bound $\mathbb{E}_{i_k} \|\nabla f_{i_k}(w_k)\|^2 \leq a(f(w_k) - f(w^*))$ with $a > 0$ (see Lemma 4 of the Appendix for the proof). This bound on the variance of the gradient results in a r.h.s. which is independent of i_k and, in the convex and strongly convex cases, it can be used to replace the SGC (see Fan et al. [2023] for more details).

As previously stated, our algorithm does not employ a constant learning rate η , but the step size η_k is instead determined at each iteration k by a line search method. Given an initial step size $\eta_{k,0}$ and $\delta \in (0, 1)$, the Stochastic Line Search (SLS) condition [Vaswani et al., 2019] select the smallest $l_k \in \mathbb{N}$ such that $\eta_k = \eta_{k,0} \delta^{l_k}$ satisfies the following condition

$$f_{i_k}(w_k - \eta_k \nabla f_{i_k}(w_k)) \leq f_{i_k}(w_k) - c\eta_k \|\nabla f_{i_k}(w_k)\|^2, \quad (1)$$

where $c \in (0, 1)$ and $\|\cdot\|$ is the Euclidean norm. Each internal step of the line search is called backtrack since the procedure starts with the largest value $\eta_{k,0}$ and reduces (cuts) it until the condition is fulfilled. Note that (1) requires a monotone decrease of f_{i_k} . In this paper, we follow Zhang and Hager [2004] and propose to replace f_{i_k} with a nonmonotone term C_k ,

$$f_{i_k}(w_k - \eta_k \nabla f_{i_k}(w_k)) \leq C_k - c\eta_k \|\nabla f_{i_k}(w_k)\|^2, \quad (2)$$

$$C_k = \max \left\{ \tilde{C}_k; f_{i_k}(w_k) \right\}, \quad \tilde{C}_k = \frac{\xi Q_k C_{k-1} + f_{i_k}(w_k)}{Q_{k+1}}, \quad Q_{k+1} = \xi Q_k + 1,$$

where $\xi \in [0, 1]$, $C_0 = Q_0 = 0$ and $C_{-1} = f_{i_0}(w_0)$. The value \tilde{C}_k is a linear combination of the previously computed function values $f_{i_0}(w_0), \dots, f_{i_k}(w_k)$ and it ranges between the strongly nonmonotone term $\frac{1}{k} \sum_{j=0}^k f_{i_j}(w_j)$ (with $\xi = 1$) and the monotone value $f_{i_k}(w_k)$ (with $\xi = 0$). The maximum in C_k is needed to ensure the use of a value that is always greater or equal than the monotone term $f_{i_k}(w_k)$. The activation of $f_{i_k}(w_k)$ instead of \tilde{C}_k happens only in the initial iterations and it is rare in deterministic problems, but becomes more common in the stochastic case. The computation of C_k does not introduce overhead since the linear combination is accumulated in C_k .

Given $\gamma > 1$, the initial step size employed in Vaswani et al. [2019] is the following

$$\eta_{k,0} = \min \{ \eta_{k-1} \gamma^{b/M}, \eta^{\max} \}. \quad (3)$$

In this paper, we propose to use the following modified version of SPS [Loizou et al., 2021]

$$\eta_{k,0} = \min \{ \tilde{\eta}_{k,0}, \eta^{\max} \} \quad \text{with} \quad \tilde{\eta}_{k,0} := \frac{f_{i_k}(w_k) - f_{i_k}^*}{c_p \|\nabla f_{i_k}(w_k)\|^2} \quad \text{and} \quad c_p \in (0, 1). \quad (4)$$

In Loizou et al. [2021], (4) is not directly employed, but equipped with the same resetting technique (3) to control the growth of $\tilde{\eta}_{k,0}$, i.e. $\eta_{k,0} = \min \{ \tilde{\eta}_{k,0}, \eta_{k-1} \gamma^{b/M}, \eta^{\max} \}$.

Given l_{k-1} the amount of backtracks at iteration $k-1$, our newly introduced resetting technique stores this value for using it in the following iteration. In particular, to relieve the line search at iteration k from the burden of cutting the new step size l_{k-1} times, the new initial step size is pre-scaled by $\delta^{l_{k-1}}$. In fact, l_{k-1} is a good estimate for l_k (see Section E.3 of the Appendix). However, to allow the original $\eta_{k,0}$ to be eventually used non-scaled, we reduce l_{k-1} by one. We thus redefine η_k as

$$\eta_k = \eta_{k,0} \delta^{\bar{l}_k} \delta^{l_k}, \quad \text{with} \quad \bar{l}_k := \max \{ \bar{l}_{k-1} + l_{k-1} - 1, 0 \}. \quad (5)$$

In Section 5, our experiments show that thanks to (5) we can save many backtracks and reduce them to zero in the majority of the iterations. At the same time, the original $\eta_{k,0}$ is not modified and the resulting step size η_k is always a scaled version of $\eta_{k,0}$. Moreover, the presence of the -1 in (5) keeps pushing $\delta^{\bar{l}_k}$ towards zero, so that the initial step size is not cut more than necessary. Note that (5) can be combined with any initial step size and it is not limited to the case of (4).

4 Rates of Convergence

We present the first rates of convergence for nonmonotone stochastic line search methods under interpolation (see Section B of the Appendix for the proofs). The three main theorems are given under strong-convexity, convexity and the PL condition. Our results do not prove convergence only for PoNoS, but more generally for methods employing (2) and any bounded initial step size, i.e.

$$\eta_{k,0} \in [\bar{\eta}^{\min}, \eta^{\max}], \quad \text{with } \eta^{\max} > \bar{\eta}^{\min} > 0. \quad (6)$$

Many step size rules in the literature fulfill the above requirement [Berrada et al., 2020, Loizou et al., 2021, Liang et al., 2019] since when applied to non-convex DL models the step size needs to be upper bounded to achieve convergence [Bottou et al., 2018, Berrada et al., 2020].

In Theorem 1 below, we show a linear rate of convergence in the case of a strongly convex function f , with each f_{i_k} being convex. We are able to recover the same speed of convergence of Theorem 1 in Vaswani et al. [2019], despite the presence of the nonmonotone term C_k instead of $f_{i_k}(w_k)$. The challenges of the new theorem originate from studying the speed of convergence of C_k to $f(w^*)$ and from combining the two interconnected sequences $\{w_k\}$ and $\{C_k\}$. It turns out that if ξ is small enough (i.e., such that $b < (1 - \eta^{\min}\mu)$), then the presence of the nonmonotone term does not alter the speed of convergence of $\{w_k\}$ to w^* , not even in terms of constants.

Theorem 1. *Let C_k and η_k be defined in (2), with $\eta_{k,0}$ defined in (6). We assume interpolation, f_{i_k} convex, f μ -strongly convex and f_{i_k} L_{i_k} -Lipschitz smooth. Assuming $c > \frac{1}{2}$ and $\xi < \frac{1}{\left(1 + \frac{\eta^{\max}}{\eta^{\min}(2c-1)}\right)}$, we have*

$$\mathbb{E} [\|w_{k+1} - w^*\|^2 + a(C_k - f(w^*))] \leq d^k (\|w_0 - w^*\|^2 + a(f(w_0) - f(w^*))),$$

where $d := \max\{(1 - \eta^{\min}\mu), b\} \in (0, 1)$, $b := \left(1 + \frac{\eta^{\max}}{ac}\right)\xi \in (0, 1)$, $a := \eta^{\min}(2 - \frac{1}{c}) > 0$ with $\eta^{\min} := \min\{\frac{2\delta(1-c)}{L_{\max}}, \bar{\eta}^{\min}\}$.

Comparing the above result with the corresponding deterministic rate (Theorem 3.1 from Zhang and Hager [2004]), we notice that the constants of the two rates are different. In particular, the proof technique employed in Theorem 3.1 from Zhang and Hager [2004] cannot be reused in Theorem 1 since a few bounds are not valid in the stochastic case (e.g., $\|\nabla f(w_{k+1})\| \leq \|\nabla f(w_k)\|$ or $C_{k+1} \leq C_k - \|\nabla f_{i_k}(w_k)\|$). The only common aspect in these proofs is the distinction between the two different cases defining C_k (i.e., being \tilde{C}_k or $f_{i_k}(w_k)$). Moreover, in both theorems ξ needs to be small enough to allow the final constant to be less than 1.

In Theorem 2 we show a $O(\frac{1}{k})$ rate of convergence in the case of a convex function f . Interestingly, in both Theorems 1 and 2 (and also in the corresponding monotone versions from Vaswani et al. [2019]), c is required to be larger than $\frac{1}{2}$. The same lower bound is also required for achieving Q-super-linear convergence for the Newton method in the deterministic case, but it is often considered too large in practice and the default value (also in the case of first-order methods) is 0.1 or smaller [Nocedal and Wright, 2006]. In this paper, we numerically tried both values and found out that $c = 0.1$ is too small since it may indeed lead to divergence (see Section E.1 of the Appendix).

Theorem 2. *Let C_k and η_k be defined in (2), with $\eta_{k,0}$ defined in (6). We assume interpolation, f convex and f_{i_k} L_{i_k} -Lipschitz smooth. Given a constant a_1 such that $0 < a_1 < (2 - \frac{1}{c})$ and assuming $c > \frac{1}{2}$ and $\xi < \frac{a_1}{2}$, we have*

$$\mathbb{E} [f(\bar{w}_k) - f(w^*)] \leq \frac{d_1}{k} \left(\frac{1}{\eta^{\min}} \|w_0 - w^*\|^2 + a_1 (f(w_0) - f(w^*)) \right),$$

where $\bar{w}_k = \frac{1}{k} \sum_{j=0}^k w_j$, $d_1 := \frac{c}{c(2-a_1)-1} > 0$, $b_1 := \left(1 + \frac{1}{a_1 c}\right)\xi \in (0, 1]$, $\eta^{\min} := \min\{\frac{2\delta(1-c)}{L_{\max}}, \bar{\eta}^{\min}\}$.

In Theorem 3 below we prove a linear convergence rate in the case of f satisfying a PL condition. We say that a function $f : \mathbb{R}^n \rightarrow \mathbb{R}$ satisfies the PL condition if there exists $\mu > 0$ such that, $\forall w \in \mathbb{R}^n : \|\nabla f(w)\|^2 \geq 2\mu(f(w) - f(w^*))$. The proof of this theorem extends Theorem 3.6 of Loizou et al. [2021] to the use of a stochastic nonmonotone line search. Again here, the presence of a nonmonotone term does not modify the constants controlling the speed of convergence (a_2 below can be chosen arbitrarily small) as long as ξ is small enough. The conditions on c and on η^{\max} are the same as those of Theorem 3.6 of Loizou et al. [2021] (see the proof).

Theorem 3. Let C_k and η_k be defined in (2), with $\eta_{k,0}$ defined in (6). We assume interpolation, the PL condition on f and that f_{i_k} are L_{i_k} -Lipschitz smooth. Given $0 < a_2 := \frac{4\mu c(1-c) - L_{max}}{4\delta c(1-c)} + \frac{1}{2\eta^{max}}$ and assuming $\frac{2\delta(1-c)}{L_{max}} < \bar{\eta}^{min}, \eta^{max} < \frac{2\delta c(1-c)}{L_{max} - 4\mu c(1-c)}, \frac{L_{max}}{4\mu} < c < 1$ and $\xi < \frac{a_2 c}{a_2 c + L_{max}}$, we have

$$\mathbb{E} [f(w_{k+1}) - f(w^*) + a_2 \eta^{max} (C_k - f(w^*))] \leq d_2^k (1 + a_2 \eta^{max}) (f(w_0) - f(w^*))$$

where $d_2 := \min \{\nu, b_2\} \in (0, 1)$, $\nu := \eta^{max} (\frac{L_{max} - 4\mu c(1-c)}{2\delta c(1-c)} + a_2) \in (0, 1)$, $b_2 := (1 + \frac{L_{max}}{a_2 c}) \xi \in (0, 1)$.

Theorem 3 is particularly meaningful for modern neural networks because of the recent work of Liu et al. [2022]. More precisely, their Theorem 8 and Theorem 13 prove that, respectively given a wide-enough fully-connected or convolutional/skip-connected neural network, the corresponding function satisfies a local version of the PL condition. As a consequence, nonmonotone line search methods achieve linear convergence for training of non-convex neural networks if the assumptions of both Theorem 3 above and Theorem 8 from Liu et al. [2022] hold and if the initial point w_0 is close enough to w^* .

5 Experiments

In this section, we benchmark PoNoS against state-of-the-art methods for training different over-parametrized models. We focus on various deep learning architectures for multi-class image classification problems, while in Section 5.3 we consider transformers for language modelling and kernel models for binary classification. In the absence of a better estimate, we assume $f_{i_k}(w^*) = 0$ for all the experiments. Indeed the final loss is in many problems very close to 0.

Concerning datasets and architectures for the image classification task, we follow the setup by Luo et al. [2019], later employed also in Vaswani et al. [2019], Loizou et al. [2021]. In particular, we focus on the datasets MNIST, FashionMNIST, CIFAR10, CIFAR100 and SVHN, addressed with the architectures MLP [Luo et al., 2019], EfficientNet-b1 [Tan and Le, 2019], ResNet-34 [He et al., 2016], DenseNet-121 [Huang et al., 2017] and WideResNet [Zagoruyko and Komodakis, 2016]. Because of space limitation, we will not show all the experiments here, but report on the first three datasets combined respectively with the first three architectures. We refer to the Appendix for the complete benchmark (see Figures 5-16) and the implementation details (Section C). In Section C of the Appendix, we also discuss the sensitivity of the results to the selection of hyper-parameters.

In Figure 1 we compare SGD [Robbins and Monro, 1951], Adam [Kingma and Ba, 2015], SLS [Vaswani et al., 2019], SPS [Loizou et al., 2021] and PoNoS. We present train loss (log scale), test accuracy and average step size within the epoch (log scale). Note that the learning rate of SGD and Adam has been chosen through a grid-search as the one achieving the best performance on each problem. Based on Figure 1, we can make the following observations:

- PoNoS achieves the best performances both in terms of train loss and test accuracy. In particular, it often terminates by reaching a loss of 10^{-6} and it always achieves the highest test accuracy.
- SLS does not always achieve the same best accuracy as PoNoS. In terms of training loss, SLS is particularly slow on `mnist|mlp` and `fashion|effb1`, while competitive on the others. On these two problems, both SLS and SPS employ a step size that is remarkably smaller than that of PoNoS. On the same problems, SPS behaves similarly as SLS because the original Polyak step size is larger than the “smoothing/resetting” value (3), i.e., $\tilde{\eta}_{k,0} > \eta_{k-1} \gamma^{b/M}$ and thus the step size is controlled by (3). On the other hand, the proposed nonmonotone line search selects a larger step size, achieving faster convergence and better generalization [Nacson et al., 2022].
- SLS encounters some cancellation errors (e.g., around epoch 120 in `cifar10|resnet34`) that lead the step size to be reduced drastically, sometimes reaching values below 10^{-7} . These events are caused by the fact that $f_{i_k}(w_k)$ and $f_{i_k}(w_{k+1})$ became numerically identical. Thanks to the nonmonotone term C_k replacing $f_{i_k}(w_k)$, PoNoS avoids cancellations errors by design.
- SGD, Adam and SPS never achieve the best test accuracy nor the best training loss. In accordance with the results in Vaswani et al. [2019], the line-search-based algorithms outperform the others.

Because of space limitation, we defer the comparison between PoNoS and its monotone counterpart to the Appendix (Section E.2). There we show that PoNoS outperforms the other line search techniques, including a tractable stochastic adaptation of the method by Grippo et al. [1986].

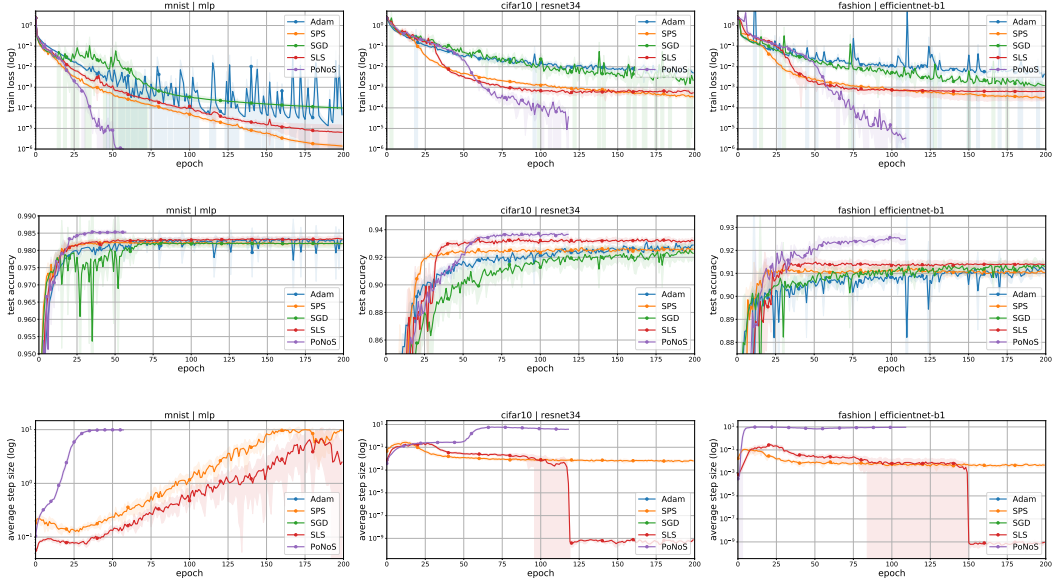


Figure 1: Comparison between the proposed method (PoNoS) and the-state-of-the-art. Each column focus on a dataset. First row: train loss. Second row: test accuracy. Third row: step size.

5.1 A New Resetting Technique

In this subsection, we compare different initial step sizes and resetting techniques. We fix the line search to be (2), but similar comments can be made on (1) (see the Section D.2 of the Appendix). In Figure 2 we compare PoNoS and PoNoS_reset0 (without (5)) with zhang_reset2 (initial step size (3)) and:

- zhang_reset3: $\eta_{k,0} = \eta_{k-1} \frac{\|\nabla f_{i_{k-1}}(w_{k-1})\|^2}{\|\nabla f_{i_k}(w_k)\|^2}$, adapted to SGD from Nocedal and Wright [2006],
- zhang_reset4: $\eta_{k,0} = \frac{2(f_{i_{k-1}}(w_{k-1}) - f_{i_{k-1}}(w_k))}{\|\nabla f_{i_{k-1}}(w_{k-1})\|}$. adapted to SGD from Nocedal and Wright [2006],
- zhang_every2: same as PoNoS_reset0, but a new step is computed only every 2 iterations.

In Figure 2, we report train loss (log scale), the total amount of backtracks per epoch and the average step size within the epoch (log scale). From Figure 2, we can make the following observations:

- PoNoS and PoNoS_reset0 achieve very similar performances. In fact, the two algorithms yield step sizes that are almost always overlapping. An important difference between PoNoS_reset0 and PoNoS can be noticed in the amount of backtracks that the two algorithms require. The plots show a sum of $\frac{M}{b}$ elements, with $\frac{M}{b} = 391$ or 469 depending on the problem and PoNoS's line hits exactly this value. This means that PoNoS employs a median of 1 backtrack per iteration for the first 5-25 epochs, while PoNoS_reset0 needs more backtracks in this stage (around 1500-3000 per-epoch, see Section D.2 of the Appendix). After this initial phase, both PoNoS_reset0 and PoNoS reduce the amount of backtracks until it reaches a (almost) constant value of 0.
- zhang_every2 does not achieve the same good performance as PoNoS or PoNoS_reset0. The common belief that step sizes can be used in many subsequent iterations does not find confirmation here. In fact, zhang_every2 shows that we cannot skip the application of a line search if we want to maintain the same good performances.
- All the other initial step sizes achieve poor performances on both train loss and test accuracy. In many cases, the algorithms yield step sizes (also before the line search) that are too small w.r.t. (4).

5.2 Time Comparison

In this subsection, we show runtime comparisons corresponding to Figure 1. In the first row of Figure 3, we plot the train loss as in the first row of Figure 1. However, the x -axis of Figure 3 measures the cumulative epoch time of the average of 5 different runs of the same algorithm with different

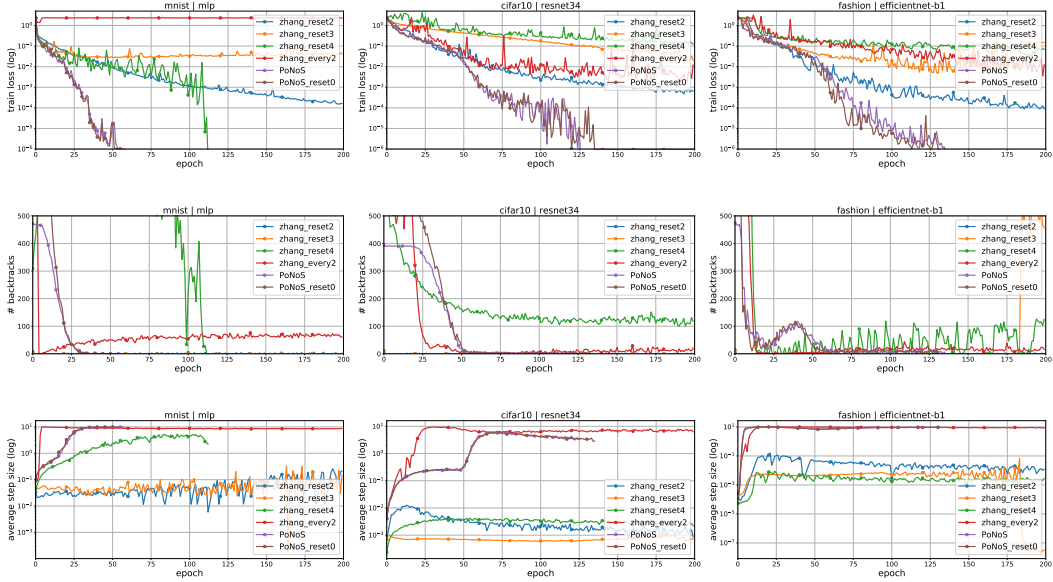


Figure 2: Comparison between different initial step sizes and resetting techniques. Each column focus on a dataset. First row: train loss. Second row: # backtracks. Third row: step size.

seeds. In the second row of Figure 3, we report the runtime per-epoch (with shaded error bars) on the y -axis and epochs on the x -axis. From Figures 1 and 3, it is clear that PoNoS is not only faster than the other methods in terms of epochs but also in terms of total computational time. In particular, PoNoS is faster than SGD, despite the fact the second achieves the lowest per-epoch time. Again from the second row of Figure 3, we can observe that PoNoS’s per-epoch time makes a transition from the phase of a median of 1 backtrack (first 5-25 epochs) to the phase of a median of 0 backtracks where its time is actually overlapping with that of SLS (always a median of 0 backtracks). In the first case, PoNoS requires less than twice the time of SGD, and in the second, this time is lower than 1.5 that of SGD. Given these measures, PoNoS becomes faster than SGD/Adam in terms of per-epoch time as soon as a grid-search (or any other hyper-parameter optimization) is employed to select the best-performing learning rate.

To conclude, let us recall that any algorithm based on a stochastic line search always requires one additional forward pass if compared with SGD. In fact, both $f_{i_k}(w_k)$ and $f_{i_k}(w_{k+1})$ are computed at each k and each backtrack requires one additional forward pass. On the other hand, if we consider that one backward pass costs roughly two forward passes and that SGD needs one forward and one backward pass, any additional forward pass costs roughly one-third of SGD. These rough calculations have been verified in Section E.6 of the Appendix, where we profiled the single iteration of PoNoS. Following these calculations and referring to the two phases of Figure 3, one iteration of PoNoS only costs $\frac{5}{3}$ that of SGD in the first phase and $\frac{4}{3}$ in the second.

5.3 Experiments for Convex Losses and for Transformers

As a last benchmark, we take into account a set of convex problems from Vaswani et al. [2019], Loizou et al. [2021] and the transformers [Vaswani et al., 2017] trained from scratch in Kunstner et al. [2023]. In Figure 4 we show one convex problem (first column) and two transformers (last two column). We leave the fine-tuning of transformers to future works. Our experiments take into account binary classification problems addressed with a RBF kernel model without regularization. We show the results achieved on the dataset mushrooms, while leaving those on ijcn, rcv1 and w8a to Section D.4 of the Appendix. Given the high amount of iterations, the smoothed version of the train loss will be reported. The test accuracy is also only reported in Section D.4 since (almost) all the methods achieve the best test accuracy in all the problems within the first few iterations. From the left subplot of Figure 4, we can observe that PoNoS obtains very good performances also in this setting (see Appendix). In Figure 4, PoNoS achieves a very low train loss (10^{-4}) within the first 200 iterations. Only SLS is able to catch up, but this takes 6 times the iterations of PoNoS. On this problem, SLS is

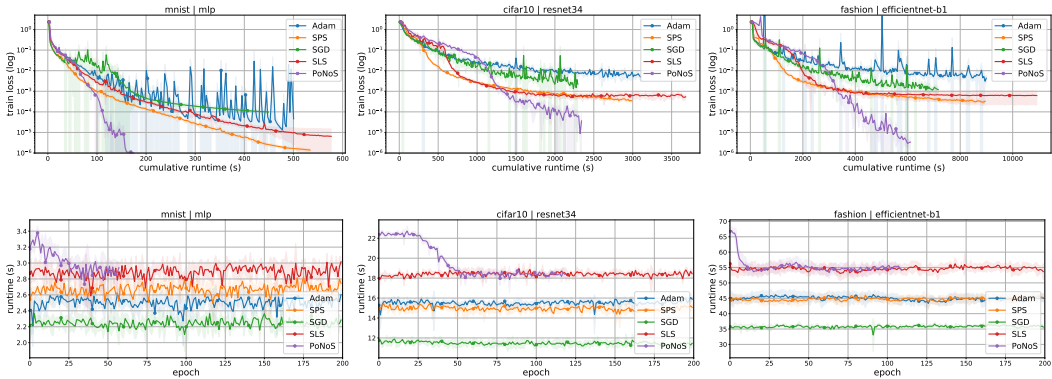


Figure 3: Time comparison (s) between the proposed method (PoNoS) and the state-of-the-art. Each column focus on a dataset. First row: train loss vs runtime. Second row: epoch runtime.

the only method reaching the value (10^{-6}). The methods SLS and SPS behave very similarly on all the datasets (see the Appendix) since in both cases (3) controls the step size. As clearly shown by the comparison with PoNoS, this choice is suboptimal and the Polyak step size is faster. Because of (3), both SLS and SPS encounter slow convergence issues in many of problems of this setting. As in Figure 1, SGD and Adam are always slower than PoNoS.

We consider training transformers on language modeling datasets. In particular, we train a Transformer Encoder [Vaswani et al., 2017] on PTB [Marcus et al., 1993] and a Transformer-XL [Dai et al., 2019] on Wikitext2 [Merity et al., 2017]. In contrast to the case of convolutional neural networks, the most popular method for training transformers is Adam and not SGD [Pan and Li, 2022, Kunstner et al., 2023]. For this reason, we use a preconditioned version of PoNoS, SLS, and SPS (respectively PoNoS_prec, SLS_prec, and SPS_prec, see Section D.5 of the Appendix for details). In fact, Adam can be considered a preconditioned version of SGD with momentum [Vaswani et al., 2020]. As in Kunstner et al. [2023], we focus on the training procedure and defer the generalization properties to the Appendix. From Figure 4, we can observe that the best algorithms in this setting are preconditioned-based and not SGD-based, in accordance with the literature. Moreover, PoNoS_prec achieves similar performances as Adam’s. In particular from the central subplot of Figure 4, we observe that PoNoS_prec is the only algorithm as fast as Adam, while all the others have difficulties achieving loss below 1. Taking the right subplot of Figure 4 into account, we can notice that PoNoS_prec is slower than Adam on this problem. On the other hand, there is not one order of difference between the two final losses (i.e., ~ 1.5 points). Moreover, we should keep in mind that Adam’s learning rate has been fine-tuned separately for each problem, while PoNoS_prec has been used off-the-shelf.

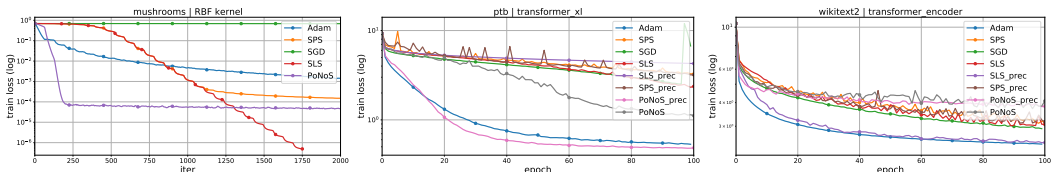


Figure 4: Train loss comparison between the new method (PoNoS) and the state-of-the-art on convex kernel models (first column) and transformers (last two columns).

6 Conclusion

In this work, we showed that modern DL models can be efficiently trained by nonmonotone line search methods. More precisely, nonmonotone techniques have been shown to outperform the monotone line searches existing in the literature. A stochastic Polyak step size with resetting has been employed as the initial step size for the nonmonotone line search, showing that the combined method is faster than the version without line search. Moreover, we presented the first runtime comparison

between line-search-based methods and SGD/Adam. The results show that the new line search is overall computationally faster than the state-of-the-art. A new resetting technique is developed to reduce the amount of backtracks to almost zero on average, while still maintaining a large initial step size. To conclude, the similar behavior of SLS_prec and Adam on the rightmost subplot of Figure 4 suggests that other initial step sizes might also be suited for training transformers. We leave such exploration (e.g., a stochastic BB like in Tan et al. [2016], Liang et al. [2019]) to future works.

We proved three convergence rate results for stochastic nonmonotone line search methods under interpolation and under either strong-convexity, convexity, or the PL condition. Our theory matches its monotone counterpart despite the use of a nonmonotone term. In the future, we plan to explore the conditions of the theorems in Liu et al. [2022] and to study a bridge between their local PL results and our global PL assumption. To conclude, it is worth mentioning that nonmonotone line search methods might be connected to the edge of stability phenomenon described in Cohen et al. [2021], because of the very similar behavior they induce in the decrease of (deterministic) objective functions. However, a rigorous study remains for future investigations.

Acknowledgments

The work was conducted within the KI-Starter project “Robustness and Generalization in Training Deep Neural Networks” funded by the Ministry of Culture and Science Nordrhein-Westfalen, Germany and partially supported by the Canada CIFAR AI Chair Program.

References

- Larry Armijo. Minimization of functions having lipschitz continuous first partial derivatives. *Pacific Journal of Mathematics*, 16(1):1–3, 1966. Cited on 1
- Hilal Asi and John C Duchi. The importance of better models in stochastic optimization. *Proceedings of the National Academy of Sciences*, 116(46):22924–22930, 2019. Cited on 2
- Jonathan Barzilai and Jonathan M Borwein. Two-point step size gradient methods. *IMA Journal of Numerical Analysis*, 8(1):141–148, 1988. Cited on 2
- Atilim Gunes Baydin, Robert Cornish, David Martinez Rubio, Mark Schmidt, and Frank Wood. Online learning rate adaptation with hypergradient descent. In *International Conference on Learning Representations*, 2017. Cited on 1
- Stefania Bellavia, Natasa Krejic, Benedetta Morini, and Simone Rebegoldi. A stochastic first-order trust-region method with inexact restoration for finite-sum minimization. *arXiv preprint arXiv:2107.03129*, 2021. Cited on 2, 3
- Leonard Berrada, Andrew Zisserman, and M Pawan Kumar. Training neural networks for and by interpolation. In *International Conference on Machine Learning*, pages 799–809. PMLR, 2020. Cited on 2, 5
- E. G. Birgin, J. M. Martínez, and M. Raydan. Nonmonotone spectral projected gradient methods on convex sets. *SIAM Journal on Optimization*, 10(4):1196–1211, 2000. Cited on 2
- R. Bollapragada, D. Mudigere, J. Nocedal, H.-J.M. Shi, and P.T.P. Tang. A progressive batching L-BFGS method for machine learning. In *International Conference on Machine Learning*, volume 2, pages 989–1013, 2018. Cited on 1
- Léon Bottou, Frank E Curtis, and Jorge Nocedal. Optimization methods for large-scale machine learning. *SIAM Review*, 60(2):223–311, 2018. Cited on 4, 5
- Chih-Chung Chang and Chih-Jen Lin. LIBSVM: A library for support vector machines. *ACM Transactions on Intelligent Systems and Technology*, 2:27:1–27:27, 2011. Cited on 25
- Jeremy Cohen, Simran Kaur, Yuanzhi Li, J Zico Kolter, and Ameet Talwalkar. Gradient descent on neural networks typically occurs at the edge of stability. In *International Conference on Learning Representations*, 2021. Cited on 1, 10

- Yu-Hong Dai. On the nonmonotone line search. *Journal of Optimization Theory and Applications*, 112(2):315–330, 2002. Cited on 3
- Zihang Dai, Zhilin Yang, Yiming Yang, Jaime G Carbonell, Quoc Le, and Ruslan Salakhutdinov. Transformer-xl: Attentive language models beyond a fixed-length context. In *Proceedings of the 57th Annual Meeting of the Association for Computational Linguistics*, pages 2978–2988, 2019. Cited on 9, 25, 29
- John Duchi, Elad Hazan, and Yoram Singer. Adaptive subgradient methods for online learning and stochastic optimization. *Journal of Machine Learning Research*, 12(7), 2011. Cited on 1
- Chen Fan, Christos Thrampoulidis, and Mark Schmidt. Fast convergence of random reshuffling under over-parameterization and the polyak-\l ojasiewicz condition. *arXiv preprint arXiv:2304.00459*, 2023. Cited on 4
- MC Ferris and S Lucidi. Nonmonotone stabilization methods for nonlinear equations. *Journal of Optimization Theory and Applications*, 81(1):53–71, 1994. Cited on 1
- Robert M Gower, Aaron Defazio, and Michael Rabbat. Stochastic Polyak stepsize with a moving target. *arXiv preprint arXiv:2106.11851*, 2021. Cited on 2
- Robert M Gower, Mathieu Blondel, Nidham Gazagnadou, and Fabian Pedregosa. Cutting some slack for SGD with adaptive polyak stepsizes. *arXiv preprint arXiv:2202.12328*, 2022. Cited on 2
- Geovani N Grapiglia and Ekkehard W Sachs. A generalized worst-case complexity analysis for non-monotone line searches. *Numerical Algorithms*, 87:779–796, 2021. Cited on 3
- Luigi Grippo, Francesco Lampariello, and Stefano Lucidi. A nonmonotone line search technique for Newton’s method. *SIAM Journal on Numerical Analysis*, 23(4):707–716, 1986. Cited on 1, 2, 3, 6, 30
- Sajad Fathi Hafshejani, Daya Gaur, Shahadat Hossain, and Robert Benkoczi. Fast armijo line search for stochastic gradient descent. *Research Square preprint <https://doi.org/10.21203/rs.3.rs-2285238/v1>*, 2023. Cited on 2, 3, 30
- Kaiming He, Xiangyu Zhang, Shaoqing Ren, and Jian Sun. Deep residual learning for image recognition. In *Proceedings of the IEEE conference on computer vision and pattern recognition*, pages 770–778, 2016. Cited on 3, 6, 25
- Gao Huang, Zhuang Liu, Laurens Van Der Maaten, and Kilian Q Weinberger. Densely connected convolutional networks. In *Proceedings of the IEEE conference on computer vision and pattern recognition*, pages 4700–4708, 2017. Cited on 3, 6, 25
- Nitish Shirish Keskar and George Saon. A nonmonotone learning rate strategy for sgd training of deep neural networks. In *2015 IEEE International Conference on Acoustics, Speech and Signal Processing (ICASSP)*, pages 4974–4978. IEEE, 2015. Cited on 2
- D.P. Kingma and J.L. Ba. Adam: A method for stochastic optimization. In *International Conference on Learning Representations*, 2015. Cited on 6
- Nataša Krejić and Nataša Krklec Jerinkić. Nonmonotone line search methods with variable sample size. *Numerical Algorithms*, 68(4):711–739, 2015. Cited on 2, 3
- Nataša Krejić and Nataša Krklec Jerinkić. Spectral projected gradient method for stochastic optimization. *Journal of Global Optimization*, 73(1):59–81, 2019. Cited on 2, 3
- Alex Krizhevsky and Geoffrey Hinton. Learning multiple layers of features from tiny images. In *Tech. rep. University of Toronto*, 2009. Cited on 25
- Frederik Kunstner, Jacques Chen, Jonathan Wilder Lavington, and Mark Schmidt. Noise is not the main factor behind the gap between sgd and adam on transformers, but sign descent might be. In *The Eleventh International Conference on Learning Representations*, 2023. Cited on 8, 9, 29

- Nicolas Le Roux, Mark Schmidt, and Francis Bach. A stochastic gradient method with an exponential convergence rate for finite training sets. *Advances in neural information processing systems*, 25, 2012. Cited on 2
- Yann LeCun, Léon Bottou, Yoshua Bengio, and Patrick Haffner. Gradient-based learning applied to document recognition. *Proceedings of the IEEE*, 86(11):2278–2324, 1998. Cited on 25
- Donghui Li and Masao Fukushima. A globally and superlinearly convergent Gauss–Newton-based BFGS method for symmetric nonlinear equations. *SIAM Journal on Numerical Analysis*, 37(1): 152–172, 1999. Cited on 2
- Shuang Li, William J Swartworth, Martin Takáč, Deanna Needell, and Robert M Gower. SP2: A second order stochastic Polyak method. *arXiv preprint arXiv:2207.08171*, 2022. Cited on 2
- Jinxu Liang, Yong Xu, Chenglong Bao, Yuhui Quan, and Hui Ji. Barzilai-Borwein-based adaptive learning rate for deep learning. *Pattern Recognition Letters*, 128:197–203, 2019. Cited on 5, 10
- Chaoyue Liu, Libin Zhu, and Mikhail Belkin. Loss landscapes and optimization in over-parameterized non-linear systems and neural networks. *Applied and Computational Harmonic Analysis*, 59: 85–116, 2022. Cited on 2, 3, 6, 10
- Nicolas Loizou, Sharan Vaswani, Issam Hadj Laradji, and Simon Lacoste-Julien. Stochastic polyak step-size for sgd: An adaptive learning rate for fast convergence. In *International Conference on Artificial Intelligence and Statistics*, pages 1306–1314. PMLR, 2021. Cited on 2, 3, 4, 5, 6, 8, 16, 26, 32
- L. Luo, Y. Xiong, Y. Liu, and X. Sun. Adaptive gradient methods with dynamic bound of learning rate. In *International Conference on Learning Representations*, 2019. Cited on 1, 6, 25
- Maren Mahsereci and Philipp Hennig. Probabilistic line searches for stochastic optimization. *The Journal of Machine Learning Research*, 18(1):4262–4320, 2017. Cited on 1, 3
- Mitchell Marcus, Beatrice Santorini, and Mary Ann Marcinkiewicz. Building a large annotated corpus of english: The Penn Treebank. *Computational Linguistics 19.2*, pages 313–330, 1993. Cited on 9, 25
- Si Yi Meng, Sharan Vaswani, Issam Hadj Laradji, Mark Schmidt, and Simon Lacoste-Julien. Fast and furious convergence: Stochastic second order methods under interpolation. In *International Conference on Artificial Intelligence and Statistics*, pages 1375–1386. PMLR, 2020. Cited on 3
- Stephen Merity, Caiming Xiong, James Bradbury, and Richard Socher. Pointer sentinel mixture models. In *International Conference on Learning Representations*, 2017. Cited on 9, 25
- Maximus Mutschler and Andreas Zell. Parabolic approximation line search for DNNs. *Advances in Neural Information Processing Systems*, 33:5405–5416, 2020. Cited on 1
- Mor Shpigel Nacson, Kavya Ravichandran, Nathan Srebro, and Daniel Soudry. Implicit bias of the step size in linear diagonal neural networks. In *International Conference on Machine Learning*, pages 16270–16295. PMLR, 2022. Cited on 1, 6
- Yuval Netzer, Tao Wang, Adam Coates, Alessandro Bissacco, Bo Wu, and Andrew Y Ng. Reading digits in natural images with unsupervised feature learning. In *NIPS Workshop on Deep Learning and Unsupervised Feature Learning*, 2011. Cited on 25
- Jorge Nocedal and Stephen Wright. *Numerical optimization*. Springer Science & Business Media, 2006. Cited on 1, 5, 7, 26, 27, 30
- Yan Pan and Yuanzhi Li. Toward understanding why Adam converges faster than SGD for transformers. In *Optimization for Machine Learning (NeurIPS Workshop)*, 2022. Cited on 9
- Courtney Paquette and Katya Scheinberg. A stochastic line search method with convergence rate analysis. *arXiv preprint arXiv:1807.07994*, 2018. Cited on 1, 3

- Adam Paszke, Sam Gross, Francisco Massa, Adam Lerer, James Bradbury, Gregory Chanan, Trevor Killeen, Zeming Lin, Natalia Gimelshein, Luca Antiga, et al. Pytorch: An imperative style, high-performance deep learning library. In *Advances in neural information processing systems*, pages 8026–8037, 2019. Cited on 25, 26
- Vassilis P Plagianakos, George D Magoulas, and Michael N Vrahatis. Deterministic nonmonotone strategies for effective training of multilayer perceptrons. *IEEE Transactions on Neural Networks*, 13(6):1268–1284, 2002. Cited on 2
- Boris Teodorovich Polyak. Minimization of unsmooth functionals. *USSR Computational Mathematics and Mathematical Physics*, 9(3):14–29, 1969. Cited on 2
- M. Raydan. The Barzilai and Borwein gradient method for the large scale unconstrained minimization problem. *SIAM Journal on Optimization*, 7(1):26–33, 1997. Cited on 2
- Herbert Robbins and Sutton Monro. A stochastic approximation method. *The Annals of Mathematical Statistics*, pages 400–407, 1951. Cited on 1, 6
- Mark Schmidt and Nicolas Le Roux. Fast convergence of stochastic gradient descent under a strong growth condition. *arXiv preprint arXiv:1308.6370*, 2013. Cited on 2
- Conghui Tan, Shiqian Ma, Yu-Hong Dai, and Yuqiu Qian. Barzilai-Borwein step size for stochastic gradient descent. In *Advances in Neural Information Processing Systems*, pages 685–693, 2016. Cited on 10
- Mingxing Tan and Quoc Le. Efficientnet: Rethinking model scaling for convolutional neural networks. In *International conference on machine learning*, pages 6105–6114. PMLR, 2019. Cited on 6, 25
- Tuyen Trung Truong and Hang-Tuan Nguyen. Backtracking gradient descent method and some applications in large scale optimisation. Part 2: Algorithms and experiments. *Applied Mathematics & Optimization*, 84(3):2557–2586, 2021. Cited on 1
- Tuyen Trung Truong and Tuan Hang Nguyen. Backtracking gradient descent method for general C^1 functions, with applications to deep learning. *arXiv preprint arXiv:1808.05160*, 2018. Cited on 1
- Ashish Vaswani, Noam Shazeer, Niki Parmar, Jakob Uszkoreit, Llion Jones, Aidan N Gomez, Łukasz Kaiser, and Illia Polosukhin. Attention is all you need. *Advances in neural information processing systems*, 30, 2017. Cited on 3, 8, 9, 25
- Sharan Vaswani, Aaron Mishkin, Issam Laradji, Mark Schmidt, Gauthier Gidel, and Simon Lacoste-Julien. Painless stochastic gradient: Interpolation, line-search, and convergence rates. In *Advances in Neural Information Processing Systems*, pages 3732–3745, 2019. Cited on 1, 2, 3, 4, 5, 6, 8, 16, 17, 26, 29, 30
- Sharan Vaswani, Issam Laradji, Frederik Kunstner, Si Yi Meng, Mark Schmidt, and Simon Lacoste-Julien. Adaptive gradient methods converge faster with over-parameterization (but you should do a line-search). *arXiv preprint arXiv:2006.06835*, 2020. Cited on 1, 9
- Yifei Wang, Zeyu Jia, and Zaiwen Wen. The search direction correction makes first-order methods faster. *arXiv preprint arXiv:1905.06507*, 2019. Cited on 2
- Yifei Wang, Zeyu Jia, and Zaiwen Wen. Search direction correction with normalized gradient makes first-order methods faster. *SIAM Journal on Scientific Computing*, 43(5):A3184–A3211, 2021. Cited on 2
- Han Xiao, Kashif Rasul, and Roland Vollgraf. Fashion-MNIST: a novel image dataset for benchmarking machine learning algorithms. *arXiv preprint arXiv:1708.07747*, 2017. Cited on 25
- Sergey Zagoruyko and Nikos Komodakis. Wide residual networks. In *British Machine Vision Conference 2016*. British Machine Vision Association, 2016. Cited on 6, 25
- Hongchao Zhang and William W Hager. A nonmonotone line search technique and its application to unconstrained optimization. *SIAM Journal on Optimization*, 14(4):1043–1056, 2004. Cited on 1, 2, 3, 4, 5, 16, 26, 31

Jingzhao Zhang, Sai Praneeth Karimireddy, Andreas Veit, Seungyeon Kim, Sashank Reddi, Sanjiv Kumar, and Suvrit Sra. Why are adaptive methods good for attention models? *Advances in Neural Information Processing Systems*, 33:15383–15393, 2020. Cited on 29

Jian L Zhou and AL Tits. Nonmonotone line search for minimax problems. *Journal of Optimization Theory and Applications*, 76(3):455–476, 1993. Cited on 2

Weijun Zhou. A short note on the global convergence of the unmodified PRP method. *Optimization Letters*, 7(6):1367–1372, 2013. Cited on 2

Appendix

Content

Appendix A The Algorithm

Appendix B Convergence Rates

Appendix B.1 Rate of Convergence for Strongly Convex Functions

Appendix B.2 Rate of Convergence for Convex Functions

Appendix B.3 Rate of Convergence for Functions Satisfying the PL Condition

Appendix B.4 Common Lemmas

Appendix B.5 The Polyak Step Size is Bounded

Appendix C Experimental details

Appendix D Plots Completing the Figures in the Main Paper

Appendix D.1 Comparison between PoNoS and the state-of-the-art

Appendix D.2 A New Resetting Technique

Appendix D.3 Time Comparison

Appendix D.4 Experiments on Convex Losses

Appendix D.5 Experiments on Transformers

Appendix E Additional Plots

Appendix E.1 Study on the Choice of c : Theory (0.5) vs Practice (0.1)

Appendix E.2 Study on the Line Search Choice: Various Nonmonotone Adaptations

Appendix E.3 Zoom in on the Amount of Backtracks

Appendix E.4 Study on the Choice of η^{\max}

Appendix E.5 Study on the Choice of c_p : Doubling the Legacy Value

Appendix E.6 Profiling PoNoS

A The Algorithm

In this section, we give the details of our proposed algorithm PoNoS.

Training machine learning models (e.g., neural networks) entails solving the following **finite sum problem**:

$$\min_{w \in \mathbb{R}^n} f(w) = \frac{1}{M} \sum_{i=1}^M f_i(w), \quad (7)$$

where w is the parameter vector and f_i corresponds to a single instance of the M points in the training set.

Given an initial step size $\eta_{k,0}$ and $\delta \in (0, 1)$, the **Stochastic (Amijo) Line Search (SLS)** [Vaswani et al., 2019] select the smallest $l_k \in \mathbb{N}$ such that $\eta_k = \eta_{k,0} \delta^{l_k}$ satisfies the following condition:

$$f_{i_k}(w_k - \eta_k \nabla f_{i_k}(w_k)) \leq f_{i_k}(w_k) - c\eta_k \|\nabla f_{i_k}(w_k)\|^2, \quad (8)$$

where $c \in (0, 1)$ and $\|\cdot\|$ is the Euclidean norm.

The newly proposed **Stochastic Zhang & Hager line search** adapted from Zhang and Hager [2004] is

$$f_{i_k}(w_k - \eta_k \nabla f_{i_k}(w_k)) \leq C_k - c\eta_k \|\nabla f_{i_k}(w_k)\|^2, \quad (9)$$

$$C_k = \max \left\{ \tilde{C}_k; f_{i_k}(w_k) \right\}, \quad \tilde{C}_k = \frac{\xi Q_k C_{k-1} + f_{i_k}(w_k)}{Q_{k+1}}, \quad Q_{k+1} = \xi Q_k + 1,$$

where $\xi \in [0, 1]$, $C_0 = Q_0 = 0$ and $C_{-1} = f_{i_0}(w_0)$.

Given $\gamma > 1$, the **resetting/smoothing technique** employed in Vaswani et al. [2019] is

$$\eta_{k,0} = \eta_{k-1} \gamma^{b/M}, \quad (10)$$

where $\gamma > 1$ and b is the mini-batch size.

Given the step size

$$\tilde{\eta}_{k,0} := \frac{f_{i_k}(w_k) - f_{i_k}^*}{c_p \|\nabla f_{i_k}(w_k)\|^2} \quad \text{and } c_p \in (0, 1), \quad (11)$$

we recall **Stochastic Polyak Step (SPS) size** from Loizou et al. [2021]

$$\eta_{k,0} = \min \left\{ \tilde{\eta}_{k,0}, \eta_{k-1} \gamma^{b/M}, \eta^{\max} \right\} \quad \text{with } \eta^{\max} > 0 \text{ and } \tilde{\eta}_{k,0} \text{ defined in (11)}, \quad (12)$$

and its **non-smoothed version** (used in Algorithm 1)

$$\eta_{k,0} = \min \left\{ \tilde{\eta}_{k,0}, \eta^{\max} \right\} \quad \text{with } \tilde{\eta}_{k,0} \text{ defined in (11)}. \quad (13)$$

To employ our new **resetting technique**, we redefine η_k as

$$\eta_k = \eta_{k,0} \delta^{\bar{l}_k} \delta^{l_k}, \quad \text{with } \bar{l}_k := \max\{\bar{l}_{k-1} + l_{k-1} - 1, 0\}. \quad (14)$$

Algorithm 1: The POLyak NONmonotone Stochastic (PoNoS) line search method

Input: $D = \{(x_i, y_i)\}_{i=1}^M$, $w_0 \in \mathbb{R}^n$, $\eta^{\max} > 0$, $c \in (0, 1)$, $c_p \in (0, 1)$, $\delta \in (0, 1)$, $\xi \in [0, 1]$, b mini-batch size, $Q_0 = 0$, $k = 0$

```

1 for epoch = 0, 1, 2, ..., max_epoch do
2   for i = 0, 1, 2, ..., M/b do
3     sample  $i_k \subset \{1, \dots, M\} : |i_k| = b$ 
4      $\eta_{k,0} = (13)$ 
5      $l_k = 0$ 
6     if  $k=0$  then
7        $C_{-1} = f_{i_0}(w_0)$ 
8        $\tilde{C}_k = \frac{\xi Q_k C_{k-1} + f_{i_k}(w_k)}{\xi Q_{k+1}}$ 
9        $C_k = \max \left\{ \tilde{C}_k; f_{i_k}(w_k) \right\}$ 
10      while  $f_{i_k}(w_k - \eta_k \nabla f_{i_k}(w_k)) > C_k - c\eta_k \|\nabla f_{i_k}(w_k)\|^2$  do
11         $l_k = l_k + 1$ 
12         $\eta_k = \eta_{k,0} \delta^{\bar{l}_k} \delta^{l_k}$ 
13       $w_{k+1} = w_k - \eta_k \nabla f_{i_k}(w_k)$ 
14       $\bar{l}_{k+1} := \max\{\bar{l}_k + l_k - 1, 0\}$ 
15       $Q_{k+1} = \xi Q_k + 1$ 
16       $k = k + 1$ 

```

B Convergence Rates

Our results do not prove convergence only for PoNoS, but more in general for methods employing (9) as a line search and a bounded initial step size, i.e.,

$$\eta_{k,0} \in [\bar{\eta}^{\min}, \eta^{\max}], \quad \text{with } \eta^{\max} > \bar{\eta}^{\min} > 0. \quad (15)$$

The next lemma provides the possible range of η_k as a consequence of the line search technique. Thanks to the fact that we always have $C_k \geq f_{i_k}(w_k)$, Lemma 1 recovers the monotone range (see Lemma 1 in Vaswani et al. [2019]). We say that f is L -Lipschitz smooth when f is continuously differentiable with Lipschitz continuous gradient, i.e.

$$\|\nabla f(x) - \nabla f(y)\| \leq L\|x - y\| \quad \forall x, y \in \mathbb{R}^n, \quad \text{with } L > 0.$$

Lemma 1. *Let f_{i_k} be L_{i_k} -Lipschitz smooth. The range of the step size η_k returned by (9) and with $\eta_{k,0}$ defined in (15) is either*

$$\eta_k \in \begin{cases} [\bar{\eta}^{\min}, \eta^{\max}] & \text{if } l_k = 0, \\ [\eta^{\min}, \eta^{\max}] & \text{if } l_k > 0, \end{cases} \quad (16)$$

where $\eta^{\min} := \min \left\{ \frac{2\delta(1-c)}{L_{max}}, \bar{\eta}^{\min} \right\}$ and $L_{max} = \max_i L_i$.

Proof. Let us denote $g_k := \nabla f_{i_k}(w_k)$. Applying Lemma 5 below on f_{i_k} , with $y = w_k - \eta_k g_k$ and $x = w_k$ we have

$$\begin{aligned} f_{i_k}(w_k - \eta_k g_k) &\leq f_{i_k}(w_k) + g_k^T(w_k - \eta_k g_k - w_k) + \frac{\eta_k^2 L_{i_k}}{2} \|g_k\|^2 \\ &= f_{i_k}(w_k) - \left(\eta_k - \frac{\eta_k^2 L_{i_k}}{2} \right) \|g_k\|^2, \end{aligned}$$

which can be rewritten as

$$f_{i_k}(w_k - \eta_k g_k) \leq p_k(\eta), \quad \text{with } p_k(\eta) := f_{i_k}(w_k) - \left(\eta - \frac{\eta^2 L_{i_k}}{2} \right) \|g_k\|^2. \quad (17)$$

Note that (17) is valid for any η . Let us rewrite (9) as

$$f_{i_k}(w_k - \eta_k g_k) \leq q_k(\eta), \quad \text{with } q_k(\eta) := C_k - c\eta \|g_k\|^2.$$

Now, the backtracking procedure in (9) admits two possible output:

Case 1: $l_k = 0$. In this case, we have $\eta_k = \eta_{k,0}$ and thus directly $\eta_k \in [\bar{\eta}^{\min}, \eta^{\max}]$.

Case 2: $l_k > 0$. In this case, we have $\eta_k < \eta_{k,0}$ with $f_{i_k}(w_k - \frac{\eta_k}{\delta} g_k) > q_k(\frac{\eta_k}{\delta})$. Then, we have that $q_k(\frac{\eta_k}{\delta}) \leq p_k(\frac{\eta_k}{\delta})$ because $q_k(\frac{\eta_k}{\delta}) > p_k(\frac{\eta_k}{\delta})$ would lead to a contradiction. In fact

$$f_{i_k}\left(w_k - \frac{\eta_k}{\delta} g_k\right) > q_k\left(\frac{\eta_k}{\delta}\right) > p_k\left(\frac{\eta_k}{\delta}\right) \geq f_{i_k}\left(w_k - \frac{\eta_k}{\delta} g_k\right)$$

is false. Thus, it has to be $q_k(\frac{\eta_k}{\delta}) \leq p_k(\frac{\eta_k}{\delta})$, from which we get that

$$f_{i_k}(w_k) - c \frac{\eta_k}{\delta} \|g_k\|^2 \leq C_k - c \frac{\eta_k}{\delta} \|g_k\|^2 \leq f_{i_k}(w_k) - \left(\frac{\eta_k}{\delta} - \frac{\eta_k^2 L_{i_k}}{2\delta^2} \right) \|g_k\|^2$$

and consequently

$$-c \leq - \left(1 - \frac{\eta_k L_{i_k}}{2\delta} \right) \Leftrightarrow \eta_k \geq \frac{2\delta(1-c)}{L_{i_k}},$$

which leads to (16). □

One of the challenges of convergence theorems for nonmonotone line search methods is to prove that the sequence of the nonmonotone terms $\{C_k\}$ converges to $f(w^*)$. In order to achieve this, in Lemma 3 below we prove that C_k and C_{k-1} are lower-bounded by $f_{i_k}(w^*)$. Before that, we establish the following auxiliary result.

Lemma 2. *From the definition of Q_k in (9), it follows*

$$1 \leq \xi Q_k + 1 \leq \frac{1}{1-\xi}. \quad (18)$$

and

$$\frac{\xi Q_k}{\xi Q_k + 1} \leq \xi \quad (19)$$

Proof. From the definition of Q_{k+1} we have

$$1 \leq \xi Q_k + 1 =: Q_{k+1} = 1 + \sum_{j=0}^k \xi^{j+1} \leq \sum_{j=0}^{\infty} \xi^j = \frac{1}{1-\xi}.$$

which implies (18). Thus we have

$$\frac{\xi Q_k}{\xi Q_k + 1} = \frac{\xi Q_k + 1 - 1}{\xi Q_k + 1} = 1 - \frac{1}{\xi Q_k + 1} \leq 1 - \frac{1}{\frac{1}{1-\xi}} = \xi.$$

which implies (19) and concludes the proof. \square

We say that f satisfies interpolations if given $w^* \in \underset{w \in \mathbb{R}^n}{\operatorname{argmin}} f(w)$, then $w^* \in \underset{w \in \mathbb{R}^n}{\operatorname{argmin}} f_i(w) \forall 1 \leq i \leq M$.

Lemma 3. *Let C_k be defined in (9). Assuming interpolation, the following bounds hold for all $k \in \mathbb{N}$,*

$$C_k - f_{i_k}(w^*) \geq 0 \quad \forall k \quad (20)$$

and

$$C_{k-1} - f_{i_k}(w^*) \geq 0 \quad \forall k. \quad (21)$$

Proof. We will prove both statements by induction, starting with (20). For $k = 0$, interpolation yields $f_{i_0}(w_0) \geq f_{i_0}(w^*)$. Assuming now that the statement is valid for $k-1 \in \mathbb{N}_0$ (i.e., $C_{k-1} - f_{i_{k-1}}(w^*) \geq 0$), let us prove that it is valid also for k . If $\tilde{C}_k > f_{i_k}(w_k)$, we have

$$C_k - f_{i_k}(w^*) = \frac{\xi Q_k}{\xi Q_k + 1} C_{k-1} + \frac{1}{\xi Q_k + 1} f_{i_k}(w_k) - f_{i_k}(w^*) \geq \frac{\xi Q_k}{\xi Q_k + 1} f_{i_{k-1}}(w^*) + \frac{1}{\xi Q_k + 1} f_{i_k}(w_k) - f_{i_k}(w^*) = 0,$$

where we used the induction hypothesis and the fact that $f_{i_{k-1}}(w^*) = f_{i_k}(w^*)$, thanks to interpolation. If $\tilde{C}_k \leq f_{i_k}(w_k)$, from interpolation we have

$$C_k - f_{i_k}(w^*) = f_{i_k}(w_k) - f_{i_k}(w^*) \geq 0.$$

The last two inequalities prove (20). We can follow a similar path for (21). For $k = 0$, from the definition of C_{-1} , we have $C_{-1} - f_{i_0}(w^*) = f_{i_0}(w_0) - f_{i_0}(w^*) \geq 0$. Assume now that the statement is valid for $k-1 \in \mathbb{N}_0$ (i.e., $C_{k-2} - f_{i_{k-1}}(w^*) \geq 0$). Then, if $\tilde{C}_{k-1} > f_{i_{k-1}}(w_{k-1})$, we have

$$\begin{aligned} C_{k-1} - f_{i_k}(w^*) &= \frac{\xi Q_{k-1}}{\xi Q_{k-1} + 1} C_{k-2} + \frac{1}{\xi Q_{k-1} + 1} f_{i_{k-1}}(w_k) - f_{i_k}(w^*) \\ &\geq \frac{\xi Q_{k-1}}{\xi Q_{k-1} + 1} f_{i_{k-1}}(w^*) + \frac{1}{\xi Q_{k-1} + 1} f_{i_{k-1}}(w_k) - f_{i_k}(w^*) = 0, \end{aligned}$$

where we used again the induction hypothesis and the fact that $f_{i_{k-1}}(w^*) = f_{i_k}(w^*)$, thanks to interpolation. If $\tilde{C}_{k-1} \leq f_{i_{k-1}}(w_{k-1})$, from interpolation we have

$$C_{k-1} - f_{i_k}(w^*) = f_{i_{k-1}}(w_k) - f_{i_{k-1}}(w^*) \geq 0,$$

which concludes the proof. \square

The following Lemma shows the importance of the interpolation property. A similar result can be obtained by replacing the L_{i_k} -smoothness assumption with the line search condition (8) or (9) (see the proof of Theorem 1 below).

Lemma 4. *We assume interpolation and that f_{i_k} are L_{i_k} -smooth. Then, we obtain*

$$\mathbb{E}_{i_k} \|\nabla f_{i_k}(w_k)\|^2 \leq L_{max} (f(w_k) - f(w^*)),$$

where $L_{max} = \max_i L_i$.

Proof. Let $w^* \in \underset{w \in \mathbb{R}^n}{\operatorname{argmin}} f(w)$ and $w_{i_k}^* \in \underset{w \in \mathbb{R}^n}{\operatorname{argmin}} f_{i_k}(w)$. From interpolation we have that $w^* \in \underset{w \in \mathbb{R}^n}{\operatorname{argmin}} f_{i_k}(w)$, which means that $f_{i_k}(w^*) = f_{i_k}(w_{i_k}^*)$. Thus, interpolation and L_{i_k} -smoothness of f_{i_k} brings to

$$\|\nabla f_{i_k}(w_k)\|^2 \leq L_{i_k} (f_{i_k}(w_k) - f_{i_k}(w_{i_k}^*)) = L_{i_k} (f_{i_k}(w_k) - f_{i_k}(w^*)).$$

Now, by applying the conditional expectation \mathbb{E}_{i_k} on the above inequality, we obtain

$$\mathbb{E}_{i_k} \|\nabla f_{i_k}(w_k)\|^2 \leq L_{max} (f(w_k) - f(w^*)).$$

\square

B.1 Rate of Convergence for Strongly Convex Functions

In this subsection, we prove a linear rate of convergence in the case of a strongly convex function f .

Theorem 1. *Let C_k and η_k be defined in (9), with $\eta_{k,0}$ defined in (15). We assume interpolation, f_{i_k} convex, f μ -strongly convex and f_{i_k} L_{i_k} -Lipschitz smooth. If $c > \frac{1}{2}$ and $\xi < \frac{1}{\left(1 + \frac{\eta^{\max}}{\eta^{\min}(2c-1)}\right)}$, we have*

$$\mathbb{E} [\|w_{k+1} - w^*\|^2 + a(C_k - f(w^*))] \leq d^k (\|w_0 - w^*\|^2 + a(f(w_0) - f(w^*))),$$

where $d := \max \{(1 - \eta^{\min} \mu), b\} \in (0, 1)$, $b := \left(1 + \frac{\eta^{\max}}{ac}\right) \xi \in (0, 1)$, $a := \eta^{\min} \left(2 - \frac{1}{c}\right) > 0$ with η^{\min} as defined in Lemma 1.

Proof. From (9) and interpolation we obtain

$$\begin{aligned} \|w_{k+1} - w^*\|^2 &= \|w_k - \eta_k \nabla f_{i_k}(w_k) - w^*\|^2 \\ &= \|w_k - w^*\|^2 - 2\eta_k \langle \nabla f_{i_k}(w_k), w_k - w^* \rangle + \eta_k^2 \|\nabla f_{i_k}(w_k)\|^2 \\ &\leq \|w_k - w^*\|^2 - 2\eta_k \langle \nabla f_{i_k}(w_k), w_k - w^* \rangle + \frac{\eta_k}{c} (C_k - f_{i_k}(w_{k+1})) \\ &\leq \|w_k - w^*\|^2 - 2\eta_k \langle \nabla f_{i_k}(w_k), w_k - w^* \rangle + \frac{\eta_k}{c} (C_k - f_{i_k}(w^*)). \end{aligned} \quad (22)$$

Let us distinguish 2 cases: either 1) $f_{i_k}(w_k) \geq \tilde{C}_k$ and then $C_k = f_{i_k}(w_k)$, or 2) $f_{i_k}(w_k) < \tilde{C}_k$ and then $C_k = \tilde{C}_k$. Let us first analyze case 1). With $c > \frac{1}{2}$ and $a = \eta^{\min} \left(2 - \frac{1}{c}\right)$, from (22) we have

$$\begin{aligned} \|w_{k+1} - w^*\|^2 + a(C_k - f_{i_k}(w^*)) &\leq \|w_k - w^*\|^2 - 2\eta_k \langle \nabla f_{i_k}(w_k), w_k - w^* \rangle + \left(a + \frac{\eta_k}{c}\right) (C_k - f_{i_k}(w^*)) \\ &= \|w_k - w^*\|^2 - 2\eta_k \langle \nabla f_{i_k}(w_k), w_k - w^* \rangle + \frac{\eta_k}{c} (f_{i_k}(w_k) - f_{i_k}(w^*)) \\ &\quad + a (f_{i_k}(w_k) - f_{i_k}(w^*)) \\ &\leq \|w_k - w^*\|^2 + \eta^{\min} \left[-2 \langle \nabla f_{i_k}(w_k), w_k - w^* \rangle + \frac{1}{c} (f_{i_k}(w_k) - f_{i_k}(w^*))\right] \\ &\quad + a (f_{i_k}(w_k) - f_{i_k}(w^*)) \\ &= \|w_k - w^*\|^2 + \eta^{\min} \left[-2 \langle \nabla f_{i_k}(w_k), w_k - w^* \rangle + \left(\frac{a}{\eta^{\min}} + \frac{1}{c}\right) (f_{i_k}(w_k) - f_{i_k}(w^*))\right] \\ &\leq \|w_k - w^*\|^2 + 2\eta^{\min} [-\langle \nabla f_{i_k}(w_k), w_k - w^* \rangle + (f_{i_k}(w_k) - f_{i_k}(w^*))] \\ &\leq \|w_k - w^*\|^2 + 2\eta^{\min} [-\langle \nabla f_{i_k}(w_k), w_k - w^* \rangle + (f_{i_k}(w_k) - f_{i_k}(w^*))] \\ &\quad + ab(C_{k-1} - f_{i_k}(w^*)), \end{aligned}$$

where the second inequality follows from $c > \frac{1}{2}$ and from the fact that the term between square brackets is negative, since f_{i_k} is a convex function. The third inequality follows from the definition of a and the last inequality follows from (21). In the following we are going to show that the same bound can also be achieved in case 2).

Let us now analyze case 2). From (22), (18) and (19), and again from $c > \frac{1}{2}$, convexity of f_{i_k} and the definition of a , we have

$$\begin{aligned} \|w_{k+1} - w^*\|^2 + a(C_k - f_{i_k}(w^*)) &\leq \|w_k - w^*\|^2 - 2\eta_k \langle \nabla f_{i_k}(w_k), w_k - w^* \rangle + \left(a + \frac{\eta_k}{c}\right) (\tilde{C}_k - f_{i_k}(w^*)) \\ &= \|w_k - w^*\|^2 - 2\eta_k \langle \nabla f_{i_k}(w_k), w_k - w^* \rangle + \left(a + \frac{\eta_k}{c}\right) \frac{1}{\xi Q_k + 1} (f_{i_k}(w_k) - f_{i_k}(w^*)) \\ &\quad + \left(a + \frac{\eta_k}{c}\right) \frac{\xi Q_k}{\xi Q_k + 1} (C_{k-1} - f_{i_k}(w^*)) \\ &\leq \|w_k - w^*\|^2 - 2\eta_k \langle \nabla f_{i_k}(w_k), w_k - w^* \rangle + 2\eta^{\min} (f_{i_k}(w_k) - f_{i_k}(w^*)) \\ &\quad + \left(a + \frac{\eta_k}{c}\right) \xi (C_{k-1} - f_{i_k}(w^*)) \\ &\leq \|w_k - w^*\|^2 + 2\eta^{\min} [-\langle \nabla f_{i_k}(w_k), w_k - w^* \rangle + (f_{i_k}(w_k) - f_{i_k}(w^*))] \\ &\quad + \left(a + \frac{\eta_k}{c}\right) \xi (C_{k-1} - f_{i_k}(w^*)) \\ &\leq \|w_k - w^*\|^2 + 2\eta^{\min} [-\langle \nabla f_{i_k}(w_k), w_k - w^* \rangle + (f_{i_k}(w_k) - f_{i_k}(w^*))] \\ &\quad + a \left(1 + \frac{\eta^{\max}}{ac}\right) \xi (C_{k-1} - f_{i_k}(w^*)), \end{aligned}$$

where the fourth inequality follows from (16). By defining $b = \left(1 + \frac{\eta^{\max}}{ac}\right) \xi$ we can conclude that the same bound holds in both cases 1) and 2). Let us now show that $b < 1$. Under the assumption that $c > \frac{1}{2}$ and $\xi < \frac{1}{\left(1 + \frac{\eta^{\max}}{\eta^{\min}(2c-1)}\right)}$ we have

$$b = \left(1 + \frac{\eta^{\max}}{ac}\right) \xi = \left(1 + \frac{\eta^{\max}}{\eta^{\min} \left(2 - \frac{1}{c}\right) c}\right) \xi = \left(1 + \frac{\eta^{\max}}{\eta^{\min} (2c-1)}\right) \xi < 1.$$

Now, by taking expectation w.r.t. i_k on the common bound achieved in both cases 1) and 2), using $\mathbb{E}_{i_k}[\nabla f_{i_k}(w_k)] = \nabla f(w_k)$, and applying strong convexity of f we obtain

$$\begin{aligned} \mathbb{E}_{i_k} [\|w_{k+1} - w^*\|^2] + a(\mathbb{E}_{i_k}[C_k] - f(w^*)) &\leq \|w_k - w^*\|^2 + 2\eta^{\min} [-\langle \nabla f(w_k), w_k - w^* \rangle + f(w_k) - f(w^*)] \\ &\quad + ab(C_{k-1} - f(w^*)) \\ &\leq \|w_k - w^*\|^2 - 2\eta^{\min} \frac{\mu}{2} \|w_k - w^*\|^2 + ab(C_{k-1} - f(w^*)) \\ &= (1 - \eta^{\min} \mu) \|w_k - w^*\|^2 + ab(C_{k-1} - f(w^*)) \\ &\leq d (\|w_k - w^*\|^2 + a(C_{k-1} - f(w^*))), \end{aligned}$$

where $d := \max\{(1 - \eta^{\min} \mu), b\}$ and in the first inequality we used the fact that C_{k-1} does not depend on i_k . Taking the total expectation gives

$$\mathbb{E} [\|w_{k+1} - w^*\|^2 + a(C_k - f(w^*))] \leq d \mathbb{E} [\|w_k - w^*\|^2 + a(C_{k-1} - f(w^*))].$$

At this point we can use the above inequality recursively, resulting in

$$\begin{aligned} \mathbb{E} [\|w_{k+1} - w^*\|^2 + a(C_k - f(w^*))] &\leq d^k \mathbb{E} [\|w_0 - w^*\|^2 + a(C_{-1} - f(w^*))] \\ &= d^k (\|w_0 - w^*\|^2 + a(f(w_0) - f(w^*))), \end{aligned}$$

where in the last equality we have used that $C_{-1} = f_{i_0}(w_0)$. □

B.2 Rate of Convergence for Convex Functions

In this subsection, we prove a $O(\frac{1}{k})$ rate of convergence in the case of a convex function.

Theorem 2. *Let C_k and η_k be defined in (9), with $\eta_{k,0}$ defined in (15). We assume interpolation, f convex and f_{i_k} L_{i_k} -Lipschitz smooth. Given a constant a_1 such that $0 < a_1 < (2 - \frac{1}{c})$, if $c > \frac{1}{2}$ and $\xi < \frac{a_1}{2}$, we have*

$$\mathbb{E} [f(\bar{w}_k) - f(w^*)] \leq \frac{d_1}{k} \left(\frac{1}{\eta^{\min}} \|w_0 - w^*\|^2 + a_1 (f(w_0) - f(w^*)) \right),$$

where $\bar{w}_k = \frac{1}{k} \sum_{j=0}^k w_j$ and $d_1 := \frac{c}{c(2-a_1)-1} > 0$.

Proof. From (9) and interpolation we obtain

$$\begin{aligned} \|w_{k+1} - w^*\|^2 &= \|w_k - \eta_k \nabla f_{i_k}(w_k) - w^*\|^2 \\ &= \|w_k - w^*\|^2 - 2\eta_k \langle \nabla f_{i_k}(w_k), w_k - w^* \rangle + \eta_k^2 \|\nabla f_{i_k}(w_k)\|^2 \\ &\leq \|w_k - w^*\|^2 - 2\eta_k \langle \nabla f_{i_k}(w_k), w_k - w^* \rangle + \frac{\eta_k}{c} (C_k - f_{i_k}(w_{k+1})) \\ &\leq \|w_k - w^*\|^2 - 2\eta_k \langle \nabla f_{i_k}(w_k), w_k - w^* \rangle + \frac{\eta_k}{c} (C_k - f_{i_k}(w^*)). \end{aligned} \tag{23}$$

Let us distinguish 2 cases: either 1) $f_{i_k}(w_k) \geq \tilde{C}_k$ and then $C_k = f_{i_k}(w_k)$, or 2) $f_{i_k}(w_k) < \tilde{C}_k$ and then $C_k = \tilde{C}_k$. Let us first analyze case 1). From (23) we have

$$\begin{aligned} \|w_{k+1} - w^*\|^2 + \eta_k a_1 (C_k - f_{i_k}(w^*)) &\leq \|w_k - w^*\|^2 - 2\eta_k \langle \nabla f_{i_k}(w_k), w_k - w^* \rangle + \left(\eta_k a_1 + \frac{\eta_k}{c} \right) (C_k - f_{i_k}(w^*)) \\ &= \|w_k - w^*\|^2 + \eta_k \left[-2\langle \nabla f_{i_k}(w_k), w_k - w^* \rangle + \left(a_1 + \frac{1}{c} \right) (f_{i_k}(w_k) - f_{i_k}(w^*)) \right] \\ &\leq \|w_k - w^*\|^2 + \eta_k \left[-2\langle \nabla f_{i_k}(w_k), w_k - w^* \rangle + \left(a_1 + \frac{1}{c} \right) (f_{i_k}(w_k) - f_{i_k}(w^*)) \right] \\ &\quad + \eta_k a_1 b_1 (C_{k-1} - f_{i_k}(w^*)), \end{aligned}$$

where the second inequality follows from (21) and $b_1 := \left(1 + \frac{1}{a_1 c}\right) \xi > 0$. The above bound will now be proven also for case 2). From (23) we have

$$\begin{aligned}
\|w_{k+1} - w^*\|^2 + \eta_k a_1 (C_k - f_{i_k}(w^*)) &\leq \|w_k - w^*\|^2 - 2\eta_k \langle \nabla f_{i_k}(w_k), w_k - w^* \rangle + \left(\eta_k a_1 + \frac{\eta_k}{c}\right) (\tilde{C}_k - f_{i_k}(w^*)) \\
&= \|w_k - w^*\|^2 - 2\eta_k \langle \nabla f_{i_k}(w_k), w_k - w^* \rangle + \left(\eta_k a_1 + \frac{\eta_k}{c}\right) \frac{1}{\xi Q_k + 1} (f_{i_k}(w_k) - f_{i_k}(w^*)) \\
&\quad + \left(\eta_k a_1 + \frac{\eta_k}{c}\right) \frac{\xi Q_k}{\xi Q_k + 1} (C_{k-1} - f_{i_k}(w^*)) \\
&\leq \|w_k - w^*\|^2 + \eta_k \left[-2 \langle \nabla f_{i_k}(w_k), w_k - w^* \rangle + \left(a_1 + \frac{1}{c}\right) (f_{i_k}(w_k) - f_{i_k}(w^*)) \right] \\
&\quad + \eta_k a_1 \left(1 + \frac{1}{a_1 c}\right) \xi (C_{k-1} - f_{i_k}(w^*)),
\end{aligned}$$

where the second inequality follows from (18) and (19). By defining $b_1 := \left(1 + \frac{1}{a_1 c}\right) \xi$ we can conclude that the same bound can be achieved in both cases 1) and 2). Let us now show that $b_1 < 1$. From the definition of a_1 , we have $\frac{1}{c} < 2 - a_1$, thus, under the assumption $\xi < \frac{a_1}{2}$ it holds that

$$b_1 = \left(1 + \frac{1}{a_1 c}\right) \xi < \left(1 + \frac{2 - a_1}{a_1}\right) \xi = \frac{2}{a_1} \xi < 1.$$

From $b_1 < 1$, rearranging and dividing the bound found for both cases 1) and 2) by $2\eta_k$, we have the following

$$\begin{aligned}
\langle \nabla f_{i_k}(w_k), w_k - w^* \rangle &\leq \frac{1}{2\eta_k} [\|w_k - w^*\|^2 - \|w_{k+1} - w^*\|^2] + \left(\frac{a_1}{2} + \frac{1}{2c}\right) (f_{i_k}(w_k) - f_{i_k}(w^*)) \\
&\quad + \frac{a_1}{2} [(C_{k-1} - f_{i_k}(w^*)) - (C_k - f_{i_k}(w^*))].
\end{aligned}$$

Now, by taking expectation w.r.t. i_k , we obtain

$$\begin{aligned}
\langle \nabla f(w_k), w_k - w^* \rangle &\leq \mathbb{E}_{i_k} \left[\frac{1}{2\eta_k} (\|w_k - w^*\|^2 - \|w_{k+1} - w^*\|^2) \right] + \left(\frac{a_1}{2} + \frac{1}{2c}\right) (f(w_k) - f(w^*)) \\
&\quad + \frac{a_1}{2} ((C_{k-1} - f(w^*)) - (\mathbb{E}_{i_k}[C_k] - f(w^*))).
\end{aligned}$$

By convexity of f we have $(f(w_k) - f(w^*)) \leq \langle \nabla f(w_k), w_k - w^* \rangle$, thus,

$$\begin{aligned}
f(w_k) - f(w^*) &\leq \mathbb{E}_{i_k} \left[\frac{1}{2\eta_k} (\|w_k - w^*\|^2 - \|w_{k+1} - w^*\|^2) \right] + \left(\frac{a_1}{2} + \frac{1}{2c}\right) (f(w_k) - f(w^*)) \\
&\quad + \frac{a_1}{2} ((C_{k-1} - f(w^*)) - (\mathbb{E}_{i_k}[C_k] - f(w^*))).
\end{aligned}$$

Moreover, noticing that $1 - \left(\frac{a_1}{2} + \frac{1}{2c}\right) > 0$ by the definition of a_1 , we obtain

$$\begin{aligned}
f(w_k) - f(w^*) &\leq \mathbb{E}_{i_k} \left[\frac{d_1}{\eta_k} (\|w_k - w^*\|^2 - \|w_{k+1} - w^*\|^2) \right] \\
&\quad + d_1 a_1 ((C_{k-1} - f(w^*)) - (\mathbb{E}_{i_k}[C_k] - f(w^*))),
\end{aligned}$$

where $d_1 := \frac{1}{2} \frac{1}{1 - \left(\frac{a_1}{2} + \frac{1}{2c}\right)} = \frac{c}{c(2 - a_1) - 1}$. Taking the total expectation and summing from k to 0

$$\begin{aligned}
\mathbb{E} \left[\sum_{j=0}^k f(w_j) - f(w^*) \right] &\leq \mathbb{E} \left[\sum_{j=0}^k \frac{d_1}{\eta_j} (\|w_j - w^*\|^2 - \|w_{j+1} - w^*\|^2) \right] \\
&\quad + d_1 a_1 \mathbb{E} \left[\sum_{j=0}^k (C_{j-1} - f(w^*)) - (C_j - f(w^*)) \right].
\end{aligned}$$

Recalling that $\bar{w}_k = \frac{1}{k} \sum_{j=0}^k w_j$, it follows from Jensen's inequality that

$$\mathbb{E} [f(\bar{w}_k) - f(w^*)] \leq \mathbb{E} \left[\frac{1}{k} \sum_{j=0}^k f(w_j) - f(w^*) \right] = \frac{1}{k} \mathbb{E} \left[\sum_{j=0}^k (f(w_j) - f(w^*)) \right].$$

Now, putting together the last two inequalities and defining $\Delta_j := \|w_j - w^*\|^2$ and $\Gamma_j := C_j - f(w^*)$, we have

$$\begin{aligned} \mathbb{E}[f(\bar{w}_k) - f(w^*)] &\leq \frac{1}{k} d_1 \mathbb{E} \left[\sum_{j=0}^k \frac{1}{\eta_j} (\Delta_j - \Delta_{j+1}) \right] + \frac{1}{k} d_1 a_1 \mathbb{E} \left[\sum_{j=0}^k \Gamma_{j-1} - \Gamma_j \right] \\ &\leq \frac{1}{k} \frac{d_1}{\eta^{\min}} \mathbb{E}[\Delta_0 - \Delta_k] + \frac{1}{k} d_1 a_1 \mathbb{E}[\Gamma_{-1} - \Gamma_k] \\ &\leq \frac{1}{k} \frac{d_1}{\eta^{\min}} \Delta_0 + \frac{1}{k} d_1 a_1 \Gamma_{-1} = \frac{d_1}{k} \left(\frac{1}{\eta^{\min}} \|w_0 - w^*\|^2 + a_1 (f(w_0) - f(w^*)) \right), \end{aligned}$$

where the second inequality follows from the fact that $\eta_k \geq \eta^{\min}$ and from simplification of the telescopic sum and the last inequality follows from $\Delta_k, \Gamma_k > 0$ (because of (20) in case of Γ_k). \square

B.3 Rate of Convergence for Functions Satisfying the PL Condition

In this subsection, we prove a linear convergence rate in the case of f satisfying a PL condition. We say that a function $f : \mathbb{R}^n \rightarrow \mathbb{R}$ satisfies the PL condition if there exists $\mu > 0$ such that, $\forall w \in \mathbb{R}^n : \|\nabla f(w)\|^2 \geq 2\mu(f(w) - f(w^*))$. From f_{i_k} being L_{i_k} -Lipschitz smooth $\forall i_k$, it follows that f is also Lipschitz smooth. Let us call L the Lipschitz smoothness constant of f and let us note that $L \leq \frac{1}{M} \sum_{i=1}^M L_i \leq L_{max}$,

Theorem 3. *Let C_k and η_k be defined in (9), with $\eta_{k,0}$ defined in (15). We assume interpolation, the PL condition on f and that f_{i_k} are L_{i_k} -Lipschitz smooth. Given $0 < a_2 := \frac{4\mu c(1-c) - L_{max}}{4\delta c(1-c)} + \frac{1}{2\eta^{max}}$ and assuming $\frac{2\delta(1-c)}{L_{max}} < \bar{\eta}^{\min}$, $\eta^{max} < \frac{2\delta c(1-c)}{L_{max} - 4\mu c(1-c)}$, $\frac{L_{max}}{4\mu} < c < 1$ and $\xi < \frac{a_2 c}{a_2 c + L_{max}}$, we have*

$$\mathbb{E}[f(w_{k+1}) - f(w^*) + a_2 \eta^{max} (C_k - f(w^*))] \leq d_2^k (1 + a_2 \eta^{max}) (f(w_0) - f(w^*))$$

where $d_2 := \min\{\nu, b_2\} \in (0, 1)$, $\nu := \eta^{max} \left(\frac{L_{max} - 4\mu c(1-c)}{2\delta c(1-c)} + a_2 \right) \in (0, 1)$, $b_2 := \left(1 + \frac{L_{max}}{a_2 c} \right) \xi \in (0, 1)$.

Proof. From the smoothness of f we obtain

$$\begin{aligned} f(w_{k+1}) &\leq f(w_k) + \langle \nabla f(w_k), w_{k+1} - w_k \rangle + \frac{L}{2} \|w_{k+1} - w_k\|^2 \\ &= f(w_k) + \eta_k \langle \nabla f(w_k), \nabla f_{i_k}(w_k) \rangle + \frac{L\eta_k^2}{2} \|\nabla f_{i_k}(w_k)\|^2 \end{aligned}$$

We then rearrange, sum $a_2(C_k - f_{i_k}(w^*))$ on both sides and use (9), to obtain

$$\begin{aligned} \frac{f(w_{k+1}) - f(w_k)}{\eta_k} + a_2(C_k - f_{i_k}(w^*)) &\leq -\langle \nabla f(w_k), \nabla f_{i_k}(w_k) \rangle + \frac{L\eta_k}{2} \|\nabla f_{i_k}(w_k)\|^2 \\ &\quad + a_2(C_k - f_{i_k}(w^*)) \\ &\leq -\langle \nabla f(w_k), \nabla f_{i_k}(w_k) \rangle + \left(\frac{L}{2c} + a_2 \right) (C_k - f_{i_k}(w^*)), \end{aligned} \tag{24}$$

Let us now distinguish 2 cases: either 1) $f_{i_k}(w_k) \geq \tilde{C}_k$ and then $C_k = f_{i_k}(w_k)$, or 2) $f_{i_k}(w_k) < \tilde{C}_k$ and then $C_k = \tilde{C}_k$. Let us first analyze case 1). Assuming $a_2, b_2 > 0$, from (24) we have

$$\begin{aligned} \frac{f(w_{k+1}) - f(w_k)}{\eta_k} + a_2(C_k - f_{i_k}(w^*)) &\leq -\langle \nabla f(w_k), \nabla f_{i_k}(w_k) \rangle + \left(\frac{L}{2c} + a_2 \right) (f_{i_k}(w_k) - f_{i_k}(w^*)) \\ &\leq -\langle \nabla f(w_k), \nabla f_{i_k}(w_k) \rangle + \left(\frac{L}{2c} + a_2 \right) (f_{i_k}(w_k) - f_{i_k}(w^*)) \\ &\quad + a_2 b_2 (C_{k-1} - f_{i_k}(w^*)) \end{aligned}$$

where the last inequality follows from (21). The above bound will be now proven also for case 2). From (24) we have

$$\begin{aligned} \frac{f(w_{k+1}) - f(w_k)}{\eta_k} + a_2(C_k - f_{i_k}(w^*)) &\leq -\langle \nabla f(w_k), \nabla f_{i_k}(w_k) \rangle + \left(\frac{L}{2c} + a_2 \right) (\tilde{C}_k - f_{i_k}(w^*)) \\ &= -\langle \nabla f(w_k), \nabla f_{i_k}(w_k) \rangle + \left(\frac{L}{2c} + a_2 \right) \frac{1}{\xi Q_k + 1} (f_{i_k}(w_k) - f_{i_k}(w^*)) \\ &\quad + \left(\frac{L}{2c} + a_2 \right) \frac{\xi Q_k}{\xi Q_k + 1} (C_{k-1} - f_{i_k}(w^*)) \\ &\leq -\langle \nabla f(w_k), \nabla f_{i_k}(w_k) \rangle + \left(\frac{L}{2c} + a_2 \right) (f_{i_k}(w_k) - f_{i_k}(w^*)) \\ &\quad + \left(\frac{L_{max}}{2c} + a_2 \right) \xi (C_{k-1} - f_{i_k}(w^*)) \end{aligned}$$

where the second inequality follows from (18) and (19) and $L \leq L_{max}$. By defining $b_2 := \left(1 + \frac{L_{max}}{a_2 c}\right) \xi$ we can conclude that the same bound can be achieved in both cases 1) and 2). Now, by taking expectation w.r.t. i_k on the common bound achieved in both cases 1) and 2), and applying PL condition, we have

$$\begin{aligned} \mathbb{E}_{i_k} \left[\frac{f(w_{k+1}) - f(w_k)}{\eta_k} + a_2(C_k - f(w^*)) \right] &\leq -\langle \nabla f(w_k), \nabla f(w_k) \rangle + \left(\frac{L}{2c} + a_2\right) (f(w_k) - f(w^*)) \\ &\quad + a_2 b_2 (C_{k-1} - f(w^*)) \\ &\leq \left(\frac{L}{2c} + a_2 - 2\mu\right) (f(w_k) - f(w^*)) \\ &\quad + a_2 b_2 (C_{k-1} - f(w^*)), \end{aligned}$$

where in the first inequality we used the fact that C_{k-1} does not depend on i_k and $\mathbb{E}_{i_k} f_{i_k}(w^*) = f(w^*) = \mathbb{E}_{i_k} f(w^*)$. Thus,

$$\begin{aligned} \mathbb{E}_{i_k} \left[\frac{f(w_{k+1}) - f(w^*)}{\eta_k} + a_2(C_k - f(w^*)) \right] &\leq \mathbb{E}_{i_k} \left[\frac{f(w_k) - f(w^*)}{\eta_k} \right] + \left(\frac{L}{2c} + a_2 - 2\mu\right) (f(w_k) - f(w^*)) \\ &\quad + a_2 b_2 (C_{k-1} - f(w^*)) \\ &\leq \left(\frac{1}{\eta^{\min}} + \frac{L}{2c} + a_2 - 2\mu\right) (f(w_k) - f(w^*)) \\ &\quad + a_2 b_2 (C_{k-1} - f(w^*)) \end{aligned}$$

Using $\eta_k \leq \eta^{\max}$, $L \leq L_{max}$ and taking the total expectation we obtain

$$\begin{aligned} \mathbb{E} [f(w_{k+1}) - f(w^*) + a_2 \eta^{\max} (C_k - f(w^*))] &\leq \eta^{\max} \left(\frac{1}{\eta^{\min}} + \frac{L_{max}}{2c} + a_2 - 2\mu\right) \mathbb{E} [f(w_k) - f(w^*)] \\ &\quad + a_2 \eta^{\max} b_2 \mathbb{E} [C_{k-1} - f(w^*)] \end{aligned} \quad (25)$$

Defining $\nu := \eta^{\max} \left(\frac{1}{\eta^{\min}} + \frac{L_{max}}{2c} + a_2 - 2\mu\right)$, let us now show that $0 < \nu < 1$. From the assumption $\bar{\eta}^{\min} > \frac{2\delta(1-c)}{L_{max}}$, we have $\eta^{\min} = \min \left\{ \frac{2\delta(1-c)}{L_{max}}, \bar{\eta}^{\min} \right\} = \frac{2\delta(1-c)}{L_{max}}$, and then

$$\nu = \eta^{\max} \left(\frac{L_{max}}{2\delta(1-c)} + \frac{L_{max}}{2c} - 2\mu + a_2 \right) = \eta^{\max} \left(\frac{L_{max}}{2\delta c(1-c)} - 2\mu + a_2 \right) = \eta^{\max} \left(\frac{L_{max} - 4\mu c(1-c)}{2\delta c(1-c)} + a_2 \right).$$

Let $a_2 := \frac{4\mu c(1-c) - L_{max}}{4\delta c(1-c)} + \frac{1}{2\eta^{\max}}$, under the assumption $\eta^{\max} < \frac{2\delta c(1-c)}{L_{max} - 4\mu c(1-c)}$, we have

$$a_2 = \frac{4\mu c(1-c) - L_{max}}{4\delta c(1-c)} + \frac{1}{2\eta^{\max}} > \frac{4\mu c(1-c) - L_{max}}{4\delta c(1-c)} + \frac{L_{max} - 4\mu c(1-c)}{4\delta c(1-c)} = 0,$$

and thus $a_2 > 0$. Let us now use substitute a_2 in the definition of ν , to obtain

$$\nu = \eta^{\max} \left(\frac{L_{max} - 4\mu c(1-c)}{2\delta c(1-c)} + a_2 \right) = \eta^{\max} \left(\frac{L_{max} - 4\mu c(1-c)}{4\delta c(1-c)} \right) + \frac{1}{2} \quad (26)$$

Again from $\eta^{\max} < \frac{2\delta c(1-c)}{L_{max} - 4\mu c(1-c)}$ and (26), we obtain $\nu < \frac{1}{2} + \frac{1}{2} = 1$. Moreover, $L_{max} - 4\mu c(1-c) > 0$ because it is a quadratic polynomial in c , whose $\Delta < 0$ since of $\mu < L_{max}$. Thus, together with $\eta^{\max} > 0$ and $4\delta c(1-c) > 0$, from (26) we achieve $\nu > 0$. Regarding b_2 , we have $b_2 > 0$ because $a_2 > 0$. Moreover, by assuming $\xi < \frac{a_2 c}{a_2 c + L_{max}}$, it also follows that

$$b_2 := \left(1 + \frac{L_{max}}{a_2 c}\right) \xi = \frac{a_2 c + L_{max}}{a_2 c} \xi < 1.$$

At this point, we need to ensure that $\frac{2\delta(1-c)}{L_{max}} < \bar{\eta}^{\min} < \eta^{\max} < \frac{2\delta c(1-c)}{L_{max} - 4\mu c(1-c)}$ or equivalently

$$\begin{aligned} 0 &< \frac{1}{L_{max}} \left(-1 + \frac{c L_{max}}{L_{max} - 4\mu c(1-c)} \right) \\ &= \frac{1}{L_{max}} \left(\frac{c L_{max} - L_{max} + 4\mu c(1-c)}{L_{max} - 4\mu c(1-c)} \right) \\ &= \frac{1}{L_{max}} \left(\frac{-4\mu c^2 + (4\mu + L_{max})c - L_{max}}{4\mu c^2 - 4\mu c + L_{max}} \right). \end{aligned}$$

In particular, we can solve the inequality for c and find that the numerator is positive for $\frac{L_{max}}{4\mu} < c < 1$ and that the denominator is always positive since $\mu < L_{max}$ (as above).

To conclude, we can use (25) recursively from k to 0 and obtain

$$\begin{aligned} \mathbb{E} [f(w_{k+1}) - f(w^*) + a_2 \eta^{\max} (C_k - f(w^*))] &\leq d_2^k \mathbb{E} [f(w_0) - f(w^*) + a_2 \eta^{\max} (C_{-1} - f(w^*))] \\ &= d_2^k (1 + a_2 \eta^{\max}) (f(w_0) - f(w^*)) \end{aligned}$$

where $d_2 := \min \{\nu, b_2\} < 1$ and in the last equality we have used that $C_{-1} = f_{i_0}(w_0)$. \square

B.4 Common Lemmas

Lemma 5. *Let f be L -Lipschitz smooth. Then*

$$f(y) \leq f(x) + \nabla f(x)^T(y - x) + \frac{L}{2}\|y - x\|^2. \quad (27)$$

Proof. From the mean value theorem and differentiability of f we have

$$\begin{aligned} f(y) &= f(x) + \int_0^1 \nabla f((1-t)x + ty)^T(y - x) dt \\ &= f(x) + \int_0^1 \nabla f((1-t)x + ty)^T(y - x) - \nabla f(x)^T(y - x) dt + \nabla f(x)^T(y - x) \\ &\leq f(x) + \int_0^1 \|\nabla f((1-t)x + ty) - \nabla f(x)\| \cdot \|y - x\| dt + \nabla f(x)^T(y - x) \\ &\leq f(x) + \int_0^1 L\|t(y - x)\| \cdot \|y - x\| dt + \nabla f(x)^T(y - x) \\ &= f(x) + L\|y - x\|^2 \cdot \frac{t^2}{2} \Big|_0^1 + \nabla f(x)^T(y - x) \\ &= f(x) + \nabla f(x)^T(y - x) + \frac{L}{2}\|y - x\|^2, \end{aligned}$$

where the second inequality follows from the Lipschitz continuity of ∇f . □

Lemma 6. *Let f be L -Lipschitz smooth and strongly convex. Then*

$$f(x) - f(x^*) \leq \frac{1}{2\mu} \|\nabla f(x)\|^2. \quad (28)$$

Proof. From the strong convexity of f we have

$$f(y) \geq r(x, y) := f(x) + \nabla f(x)^T(y - x) + \frac{\mu}{2}\|y - x\|^2.$$

We now minimize both sides of the above inequality w.r.t. y . In particular, we differentiate $r(x, y)$ w.r.t. y and obtain

$$\frac{\partial r(x, y)}{\partial y} = \nabla f(x) + \mu(y - x) = 0 \Leftrightarrow y^* = x - \frac{1}{\mu} \nabla f(x)$$

which means that

$$r(x, y^*) = f(x) - \frac{1}{\mu} \|\nabla f(x)\|^2 + \frac{1}{2\mu} \|\nabla f(x)\|^2 = f(x) - \frac{1}{2\mu} \|\nabla f(x)\|^2.$$

Thus, since $\min_y f(y) \geq \min_y r(x, y)$, we can conclude that

$$f(x^*) \geq f(x) - \frac{1}{2\mu} \|\nabla f(x)\|^2. \quad (29)$$

□

Lemma 7. *Let f be L -Lipschitz smooth. Then*

$$\frac{1}{2L} \|\nabla f(x)\|^2 \leq f(x) - f(x^*). \quad (30)$$

Proof. We can repeat the same argument of Lemma 6 in the following inequality (obtained applying Lemma 5)

$$f(y) \leq f(x) + \nabla f(x)^T(y - x) + \frac{L}{2}\|y - x\|^2,$$

and get that

$$f(x^*) \leq f(x) - \frac{1}{2L} \|\nabla f(x)\|^2,$$

which concludes the proof. □

problem \ data	n	M	b	$\frac{M}{b}$	test size	max epochs (corr. iter.)
1	535818	60000	128	469	10000	200 (93800)
2	21282122	50000	128	391	10000	200 (78200)
3	6956298	50000	128	391	10000	200 (78200)
4	21328292	50000	128	391	10000	200 (78200)
5	7048548	50000	128	391	10000	200 (78200)
6	6525418	60000	128	469	10000	200 (93800)
7	369498	73257	128	573	26032	200 (114600)
8	112	6499	100	65	1625	35 (2275)
9	22	39992	100	400	9998	35 (14000)
10	47236	16194	100	162	4048	35 (5670)
11	300	39799	100	398	9950	35 (13930)
12	13828478	59712	64	933	/	100 (93300)
13	30725904	7296	64	114	/	100 (11400)

Table 1: Information on the problems and on some of the hyper-parameters of the algorithms. In order by column: number of parameters of the model n , number of instances of the train set M , batch size b , number of iterations ($\#$ mini-batches) in each epoch $\frac{M}{b}$, number of instances in the test set, max amount of epochs (corresponding max amount of iterations).

B.5 The Polyak Step Size is Bounded

In this subsection, we show that the Polyak step size (13) is bounded. In particular, this step is capped at $\eta^{\max} > 0$, so it is bounded from above by η^{\max} . By definition of (13), interpolation and Lemma 7 applied on f_{i_k} we get

$$\eta_{k,0} \geq \frac{f_{i_k}(w_k) - f_{i_k}^*}{c_p \|\nabla f_{i_k}(w_k)\|^2} \geq \frac{\frac{1}{2L_{i_k}} \|\nabla f_{i_k}(w_k)\|^2}{c_p \|\nabla f_{i_k}(w_k)\|^2} \geq \frac{1}{2c_p L_{max}}.$$

C Experimental Details

The PyTorch [Paszke et al., 2019] code to reproduce our results can be found at <https://github.com/leonardogalli91/PoNoS>. Also, PoNoS is there available as a `torch.optim.Optimizer`. Experiments are conducted on a machine with an NVIDIA A100 PCIe GPU with 40 GB of memory.

Problems (dataset, model):

1. MNIST, MLP (1 hidden-layer multi-layer perceptron of width 1000) [LeCun et al., 1998, Luo et al., 2019];
2. CIFAR10, ResNet-34 [Krizhevsky and Hinton, 2009, He et al., 2016];
3. CIFAR10, DenseNet-121 [Krizhevsky and Hinton, 2009, Huang et al., 2017];
4. CIFAR100, ResNet-34 [Krizhevsky and Hinton, 2009, He et al., 2016];
5. CIFAR100, DenseNet-121 [Krizhevsky and Hinton, 2009, Huang et al., 2017];
6. Fashion MNIST, EFFicientnet-B1 [Xiao et al., 2017, Tan and Le, 2019];
7. SVHN, WideResNet [Netzer et al., 2011, Zagoruyko and Komodakis, 2016];
8. mushrooms, RBF-kernel model [Chang and Lin, 2011];
9. rcv1, RBF-kernel model [Chang and Lin, 2011];
10. ijcnn, RBF-kernel model [Chang and Lin, 2011];
11. w8a, RBF-kernel model [Chang and Lin, 2011];
12. PTB, Transformer Encoder [Marcus et al., 1993, Vaswani et al., 2017];
13. Wikitext2, Transformer-XL [Dai et al., 2019, Merity et al., 2017].

All the datasets can be freely obtained respectively through the `pytorch` package (image classification), or from the LIBSVM repository [Chang and Lin, 2011] (binary classification), or from the websites <http://www.fit.vutbr.cz/~imikolov/rnnlm/simple-examples.tgz> (PTB) and <https://s3.amazonaws.com/research.metamind.io/wikitext/wikitext-2-v1.zip> (Wikitext2). In Table 1, we report a few information concerning the problems above and the hyper-parameters employed by the algorithms on that problem. In order by column, we report the number of parameters of the model n , the number of instances of the train set M , the batch size employed by the algorithms b , the number of iterations ($\#$ mini-batches) in each epoch $\frac{M}{b}$, the number of instances in the test set, the max amount of epochs and in brackets the corresponding max number of iterations. The combinations of dataset/model have been replaced by the corresponding number in the above listing.

The numerical results report various measures:

- train loss: the full-batch loss on the training set;
- test accuracy: accuracy on the test set;
- average step size: average of all the mini-batch step sizes within the epoch;

problem \ method	1	2	3	4	5	6	7	8	9	10	11	12	13
SGD	0.1	0.1	0.1	0.1	0.1	0.1	0.1	0.1	0.1	0.1	0.1	0.5	0.25
Adam	10^{-4}	10^{-3}	10^{-3}	10^{-3}	10^{-3}	10^{-3}	10^{-3}	0.1	0.1	0.1	0.1	$2.5 \cdot 10^{-4}$	$2.5 \cdot 10^{-4}$

Table 2: Learning rates for SGD and Adam obtained through a grid-search procedure.

- initial step size: average of all the mini-batch initial step sizes within the epoch;
- gradient norm: average of all the mini-batch gradient norms within the epoch;
- # backtracks: the total number of backtracking steps required within the epoch;
- runtime: wall clock time of each epoch.

Many of the plots in this paper have been created by averaging 5 runs that differ from each other only on the random seed randomizing the algorithms. The shaded error bars in the plots correspond to the standard deviation from the mean of the 5 runs.

If not specified differently, the following is the setting of hyper-parameters used for Algorithm 1

$$\delta = 0.5, \quad \xi = 1, \quad \eta^{\max} = 10, \quad c = 0.5, \quad c_p = 0.1.$$

The performance of PoNoS is not sensitive to hyper-parameters. In fact, the same values work across experiments and there is no need to fine-tune them. Most of PoNoS’s hyperparameters are set to standard values, while others are either inherited by recent papers or fixed by the theory:

- $\delta = 0.5$, classical cut of the step [Nocedal and Wright, 2006]. SLS employs an unusual value of 0.9 and this choice is connected to the use of their resetting technique (10). We checked the results of SLS with $\delta = 0.5$ and they indeed turned out to not be as good as with $\delta = 0.9$.
- $\xi = 1$, the fully nonmonotone version of Zhang and Hager [2004].
- $\eta^{\max} = 10$, very classical value [Vaswani et al., 2019, Loizou et al., 2021]. We conducted an ablation study in Section E.4, which shows that larger values of η^{\max} do not have a remarkable impact on the results. These results show that PoNoS is more robust than SLS and SPS to these changes.
- $c = 0.5$, suggested by the theory. Both our theory and that of Vaswani et al. [2019] suggest employing 0.5 for c , rather than the classical 0.1 or lower [Nocedal and Wright, 2006]. The numerical results in Section E.1 support this choice. In particular, they show in Figure 11 that $c = 0.1$ might bring PoNoS and its monotone counterpart to diverge.
- $c_p = 0.1$, half of the inherited value [Loizou et al., 2021]. In Loizou et al. [2021], the value 0.2 was suggested for SPS, however in our case, the initial step size is not the final step since the backtracking procedure might reduce this value to its half (or less). For this reason, we decided to employ a step that is initially double that of SPS. The results show that PoNoS0.1 is consistently better than PoNoS0.2 (see Section E.5). Thus, we also checked whether SPS0.1 would be consistently better than the original SPS, but this is not the case.

All the other optimizers were used with their default hyper-parameters and without any weight decay. The implementation of SGD and Adam is provided by `pytorch` [Paszke et al., 2019] and their learning rates were selected through a separate grid search on each of the problems. These values are collected in Table 2, where again the names are replaced by the above numbers. For the classification problems (1-11) the grid search was $\{10^{-1}, 10^{-2}, 10^{-3}, 10^{-4}\}$, while for training the language models we employed the larger grid $\{5, 2.5, 1\} \times \{10^{-1}, 10^{-2}, 10^{-3}, 10^{-4}\}$.

D Plots Completing the Figures in the Main Paper

D.1 Comparison between PoNoS and the state-of-the-art

See Figure 5 for the complete results relative to Figure 1 of the main paper. From Figure 5 we can additionally observe that on some problems (e.g., `cifar100|resnet34` and `cifar100|densenet121`) the step size yielded by the Polyak formula (12) is very big and grows very fast. The algorithm SPS controls this step by reducing it to (10). This step does not depend on the Polyak rule and it does not employ the local information provided by $f_{i_k}(w_k)$ and $\nabla f_{i_k}(w_k)$. Instead, it grows exponentially controlled by (10). On the other hand, the step size of PoNoS is always a scaled version of (12).

D.2 A New Resetting Technique

See Figure 6 for the complete results relative to Figure 2 of the main paper. From Figure 6, we can additionally observe that the step size yielded by PoNoS is generally small in the initial phase, it grows in the intermediate phase and reaches η^{\max} towards the end. This behavior can be also noticed in the amount of backtracks of PoNoS_reset0 in the rightmost column of Figure 6. The number of backtracks is conspicuous at the beginning, rare in the intermediate phase and (almost) zero in the local phase. On the other hand, the resetting technique introduced in PoNoS maintains the amount of backtracks to be limited by 1 per iteration (on average), while still yielding the same step size. When PoNoS_reset0 starts to reduce the amount of backtracks, also PoNoS does the same.

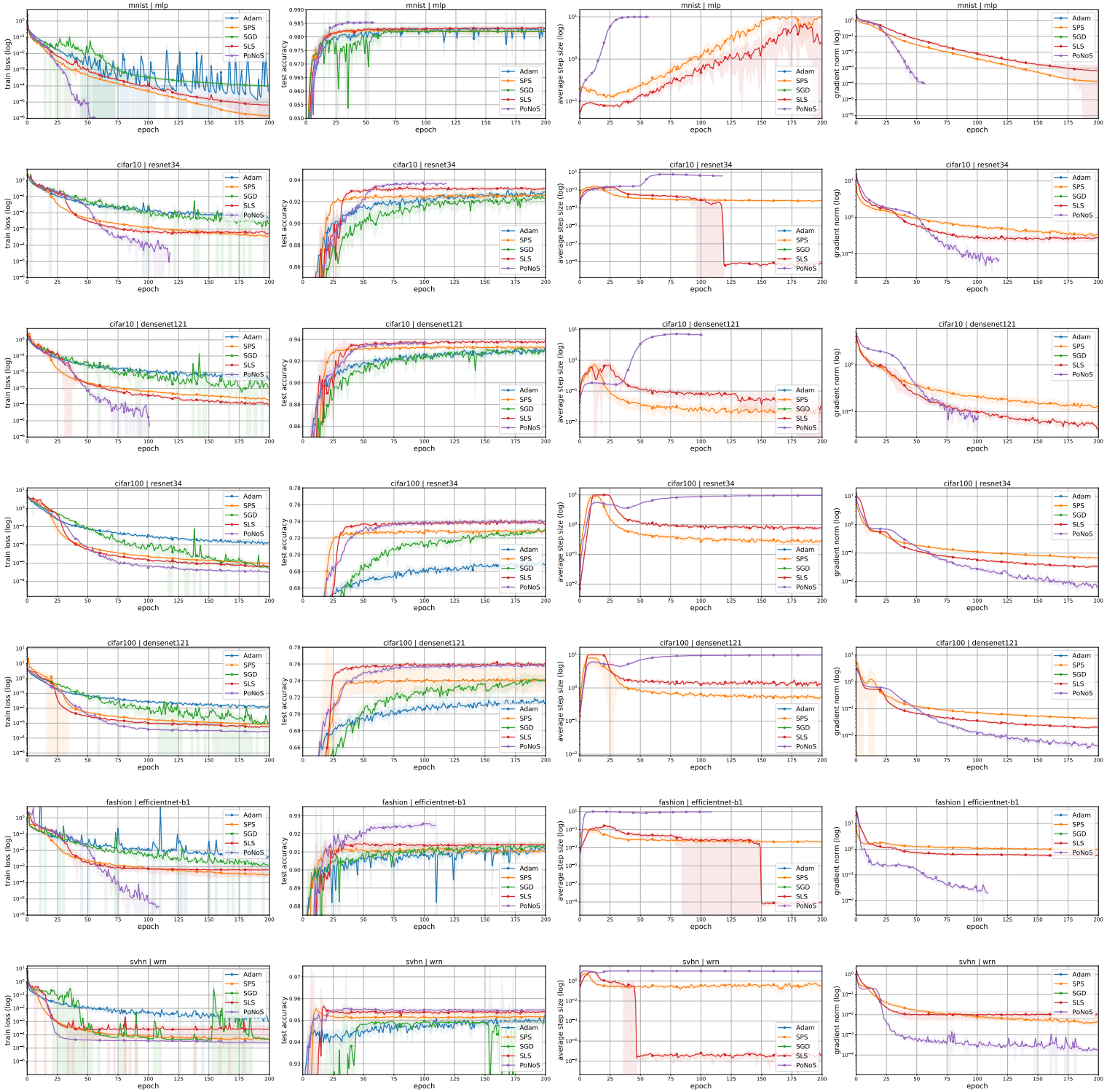


Figure 5: Comparison between the proposed method (PoNoS) and the state-of-the-art. Each row focus on a dataset/model combination. First column: train loss. Second column: test accuracy. Third column: average step size of the epoch. Fourth column: average gradient norm of the epoch.

The step size behavior described above and the corresponding amount of backtracks are in accordance with the intuition and the theory. Intuitively, a small step size allows the algorithm to proceed more cautiously in the global phase. A larger step size allows the algorithm to converge faster once it gets closer to the local phase. In fact, for achieving local Q -superlinear convergence, the theory predicts that the line search should always accept a new step size in the local phase [Nocedal and Wright, 2006].

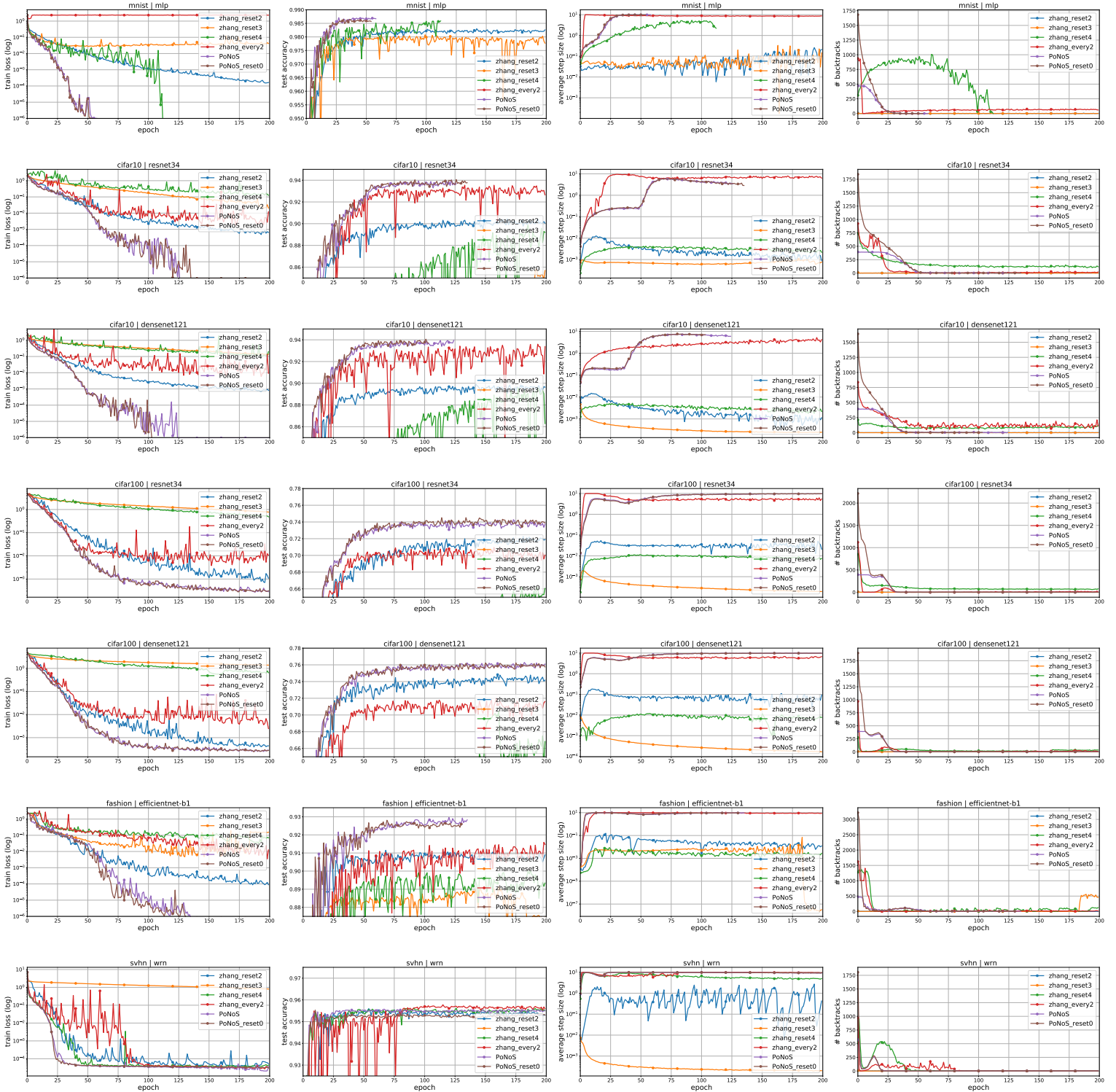


Figure 6: Comparison between different initial step sizes and resetting techniques. Each row focus on a dataset/model combination. First column: train loss. Second column: test accuracy. Third column: average step size of the epoch. Fourth column: cumulative number of backtracks in the epoch.

D.3 Time Comparison

See Figure 7 for the complete results relative to Figure 3 of the main paper. All the time measures are obtained by using the `time.time()` command from the `time` python package. The cumulative time in the x -axis of the first and second columns of Figure 7 has been computed as an average of 5 different runs. More precisely, the time of each epoch have been computed separately for the 5

runs and then averaged, so that the same average time has been assigned to each of the 5 runs. At this point, these averaged per-epoch times have been cumulated along the epochs. The shaded error bars in the plots correspond to the standard deviation from the mean of the loss/accuracy and not to the runtime. The runtime standard deviation is instead reported in the third column of Figure 7.

D.4 Experiments on Convex Losses

See Figure 8 for the complete results relative to the convex experiments of Figure 4 of the main paper. Only the training sets available in the LIBSVM library were used for these datasets. The 80% split of the data was used as a training set and 20% split as the test set. For the RBF kernel bandwidth, we employed the parameters suggested in Vaswani et al. [2019], that is $\{0.5, 0.25, 0.05, 20\}$ respectively for mushrooms, rcv1, ijcn and w8a. We did not use any bias parameter in these experiments. Furthermore, given the convexity of these problems, η^{\max} is not needed and it has been set to ∞ .

In Figure 8, the three measures are reported by iterations and not by epochs. To avoid large fluctuations in the plots, train loss and step size have been smoothed using an exponential moving average ($\beta = 0.9$). On the other hand, the test accuracy is only computed at the beginning of each epoch and the same value is reported till the next epoch. In Figure 8, we can make additional observations which are not visible in Figure 4 of the main paper:

- PoNoS achieves the lowest loss value on rcv1 and ijcn. Regarding the test accuracy, PoNoS achieves always the highest score, apart from rcv1 on which it loses 0.5 points w.r.t. SLS and SPS.
- SLS and SPS behave very similarly on all the datasets. They achieve the best accuracy on all the problems, but they are both very slow on mushrooms, rcv1 and ijcn in terms of loss. This behavior is due to (10), as it is clear from the third column of Figure 8. The step size yielded by (10) is often too small and it slowly grows exponentially through the whole optimization process. This choice is suboptimal if compared with the step size yielded by PoNoS.

D.5 Experiments on Transformers

See Figure 9 for the complete results relative to experiments on transformers of Figure 4 of the main paper. In these experiments, we followed the setup by Kunstner et al. [2023]. The word-level language modeling has been addressed with sequences of 35 or 128 tokens respectively for PTB and Wikitext2. In case of PTB, we employed a simple transformer model whose architecture consists of an 200-dimensional embedding layer, 2 transformer layers (2-head self attention, layer normalization, linear(200 × 200)-ReLU-linear(200 × 200), layer normalization) followed by a linear layer. The data processing and the implementation of the Transformer-XL follow Dai et al. [2019]. In the case of Wikitext2, the hyperparameters are set as in the ENWIK8 base experiment of Dai et al. [2019], except with the modifications of Zhang et al. [2020], using 6 layers and a target length of 128.

Since Adam is commonly known to achieve better performances than SGD on these networks [Kunstner et al., 2023], we develop a preconditioned version of PoNoS, SLS and SPS respectively called PoNoS_prec, SLS_prec, and SPS_prec. These algorithms differ from the originals in three aspects. First, they all employ a direction which is Adam without momentum ($\beta_1 = 0$). More precisely, the mini-batch gradient $\nabla f_{i_k}(w_k)$ in Step 13 of Algorithm 1 is replaced with d_k as computed below

$$\begin{aligned} g_k &= \nabla f_{i_k}(w_k) \\ v_k &= \beta_2 \cdot v_{k-1} + (1 - \beta_2) \cdot g_k^2 \\ \hat{v}_k &= v_k / (1 - \beta_2^k) \\ d_k &= -g_k / (\sqrt{\hat{v}_k} + \epsilon), \end{aligned}$$

where all the operations on vectors are to be considered component-wise, $\beta_2 \in (0, 1)$ and $\epsilon > 0$ is a small constant. We use the default values from Adam for β_2 and ϵ , that is $\beta_2 = 0.9$ and $\epsilon = 10^{-8}$. The second difference concerns the line search, as PoNoS_prec and SLS_prec exploit a condition that reflects the use of the above preconditioned direction, i.e.,

$$f_{i_k}(w_k + \eta_k d_k) \leq R_k + c \cdot \eta_k \langle d_k, \nabla f_{i_k}(w_k) \rangle = R_k - c \cdot \eta_k \sum_{j=0}^{n-1} \frac{(\nabla f_{i_k}(w_k))_j^2}{(\sqrt{\hat{v}_k} + \epsilon)_j},$$

where $(\cdot)_j$ is referring to the j -th component of the vector in brackets, and R_k is either C_k in case of PoNoS_prec or $f_{i_k}(w_k)$ in case of SLS_prec. The third difference concerns the Polyak step size, which is also computed taking into account the above directional derivative $\langle d_k, \nabla f_{i_k}(w_k) \rangle$. In particular, PoNoS_prec and SPS_prec replace (11) with the following

$$\tilde{\eta}_{k,0} := \frac{f_{i_k}(w_k) - f_{i_k}^*}{-c_p \langle d_k, \nabla f_{i_k}(w_k) \rangle}.$$

As in Kunstner et al. [2023] we focus on the training procedure, however, in the second column of Figure 9 we report the perplexity of the language model on the test. With respect to Figure 4 of the main paper, in Figure 9 we also show the gradient norm and the step size yielded by the different methods. From these plots, it is possible to notice that the range in which the step size varies is reduced if compared with that of Figure 5. This behavior depends on the dynamics of the loss and of the norm of the gradient, which are also reduced if compared with those of Figure 5. The reduced ranges of loss and gradient norm might be an issue for Polyak-based algorithms since they rely on these measures. Furthermore, the good results of SLS_prec on wiki2|encoder suggest that other initial step sizes might also be suited for training transformers. We leave such exploration to future works.

E Additional Plots

E.1 Study on the Choice of c : Theory (0.5) vs Practice (0.1)

In these experiments, we consider the constant c in (9) and (8). As described in Section 4 of the main paper, this value is required to be larger than $\frac{1}{2}$ in both Theorems 1 and 2 (and also in the corresponding monotone versions from Vaswani et al. [2019]). This value is often considered too large in practice and the default choice is 0.1 (also for SLS [Vaswani et al., 2019]) or smaller [Nocedal and Wright, 2006]. The constant c controls the weight of the sufficient decrease in the line search conditions and a smaller value of c corresponds to a looser line search. In this subsection, we numerically try both $c = 0.5$ and $c = 0.1$. In Figure 10 and 11 we compare

- `monotone|0.1`: the monotone stochastic Armijo line search (8) with $c = 0.1$.
- `monotone|0.5`: the monotone stochastic Armijo line search (8) with $c = 0.5$.
- `zhang|0.1`: the nonmonotone Zhang and Hager line search (9) with $c = 0.1$.
- `zhang|0.5`: the nonmonotone Zhang and Hager line search (9) with $c = 0.5$. This setting corresponds to PoNoS.

For all the above algorithms the initial step size is (12). From Figure 10 we can observe that:

- `zhang|0.5` (PoNoS) achieves the best performances both in terms of train loss and test accuracy. It is the only algorithm able to reduce the train loss below the threshold of 10^{-6} on the problems `cifar10|resnet34` and `cifar100|resnet34`. Apart from the case of `svhn|wrn` (where it loses less than 0.5 points w.r.t. `zhang|0.1`), it always achieves the best test accuracy.
- `monotone|0.1` and `zhang|0.1` are generally competitive in terms of training loss, but they achieve very poor generalization skills on `cifar100|resnet34` and `cifar100|densenet121`. In particular, their step size on these two problems is growing very rapidly. Already in the first epoch, the average step size is greater than 5, thanks to the fact that both algorithms are reducing the gradient norm rapidly below 1.
- The step size yielded by `zhang|0.5` starts substantially lower than those of `monotone|0.1` and `zhang|0.1`. Afterwards, the step size increases, then stabilizes, sometimes slightly decreases and finally increases again. This behavior is accomplished thanks to the combination between a larger c and a nonmonotone line search. Also the gradient norm is affected by this choice, since it does not decrease as suddenly as for `monotone|0.1` and `zhang|0.1`.
- `monotone|0.5` never achieves the best test accuracy nor the best training loss. This line search is too strict and yields step sizes that are very small in comparison to those yielded by `zhang|0.5`.

In conclusion, PoNoS (`zhang|0.5`) employs a large constant c (0.5), but it combines that with a nonmonotone line search to achieve the best middle way between strictness and tolerance.

In Figure 11 we propose the same comparison as in Figure 10, but in the case of the convex experiments of Figure 8. From Figure 11 we can observe that `zhang|0.1` and `monotone|0.1` do not obtain good performances. On both `rcv1` and `ijcnn`, these algorithms do not converge, suggesting that a large constant c is sometimes required to achieve convergence.

E.2 Study on the Line Search Choice: Various Nonmonotone Adaptations

In this subsection, we propose a comparison between various line search conditions. For the first time in this paper, we adapt different nonmonotone techniques to SGD. A straightforward adaptation of the nonmonotone line search from Grippo et al. [1986] is

$$f_{i_k}(w_k - \eta_k \nabla f_{i_k}(w_k)) \leq \max_{0 \leq j \leq W-1} f_{i_k}(w_{k-j}) - c\eta_k \|\nabla f_{i_k}(w_k)\|^2. \quad (31)$$

The nonmonotone term in (31) can be computed in two ways. Either by keeping in memory W (usually 10 or 20) previous vector weights $\{w_{k-W}, \dots, w_k\}$ and computing the current mini-batch function f_{i_k} on all of them. Or by computing all the following W mini-batch functions $\{f_{i_k}(\cdot), \dots, f_{i_{k+W}}(\cdot)\}$ on w_k . Both options are very expensive in the case of large neural networks and they should be avoided. The condition (31) is the same proposed in Hafshejani et al. [2023].

To reduce the cost of computing (31), we here propose two other stochastic adaptations of the nonmonotone line search from Grippo et al. [1986]. We name *cross-batch Grippo* the following line search condition

$$f_{i_k}(w_k - \eta_k \nabla f_{i_k}(w_k)) \leq f_{i_{k-\tilde{r}}}(w_{\tilde{r}}) - c\eta_k \|\nabla f_{i_k}(w_k)\|^2, \quad (32)$$

where \tilde{r} is a short notation for $\tilde{r}(k, i_k)$, which is the (say, largest) iteration index such that

$f_{i_{k-\tilde{r}(k, i_k)}}(w_{\tilde{r}(k, i_k)}) = \max_{0 \leq j \leq W-1} f_{i_{k-j}}(w_{k-j})$. The computation of (32) does not introduce overhead since it directly uses the function values computed in the previous iterations. However, the fact that (32) computes the maximum over different mini-batch functions $\{f_{i_{k-W}}(\cdot), \dots, f_{i_k}(\cdot)\}$ complicates the convergence analysis. We conjecture that under the interpolation assumption alone, it is not possible to achieve convergence if (32) replaces (9), not even in the strongly convex case.

We call *single-batch Grippo* the following line search condition

$$f_{i_k}(w_k - \eta_k \nabla f_{i_k}(w_k)) \leq f_{i_k}(w_{r(k, i_k)}) - c\eta_k \|\nabla f_{i_k}(w_k)\|^2, \quad (33)$$

where $r(k, i_k)$ is the (say, largest) iteration index such that $f_{i_k}(w_{r(k, i_k)}) = \max_{0 \leq j \leq W-1} f_{i_k}(w_{k-j \frac{W}{b}})$. This line search is similar to (31) since it focuses on f_{i_k} . However, it also reduces the cost of computing the nonmonotone term. In fact, given a certain set of indexes i_k ,

it exploits the function values computed in the previous epochs, without re-computing f_{i_k} . This requires saving a matrix of $M \times W$ floating-point numbers. On the other hand, to use this computational trick, the nonmonotone term can only be computed starting from the second epoch. Moreover, (33) is not computationally as cheap as (32) or (9). In particular, at every mini-batch iteration (32) requires the extraction of the $b \times W$ values corresponding to the indexes in i_k from the above-mentioned matrix and to compute the maximum over these values.

In Figure 12 we compare

- monotone: the monotone stochastic Armijo line search (8).
- cross_batch_grippo: the cross-batch nonmonotone Grippo’s line search (32) with $W = \frac{M}{b}$.
- single_batch_grippo: the single-batch nonmonotone Grippo’s line search (33) with $W = 10$.
- zhang: the nonmonotone Zhang and Hager [2004] line search adapted to the stochastic case (9). This setting corresponds to PoNoS.

For all the above algorithms the initial step size is (12). From Figure 12 we can observe that:

- zhang (PoNoS) achieves the best performances both in terms of train loss and test accuracy. Also in this case, it is the only algorithm able to reduce the train loss below the threshold of 10^{-6} on the problems `cifar10|resnet34`, `cifar10|densenet121` and `fashion|effb1`. Moreover, it always achieves the highest test accuracy. In `fashion|effb1` it is not as fast as `cross_batch_grippo` and `single_batch_grippo`.
- `single_batch_grippo` achieves similar performances as zhang. However, it does not always reach the same test accuracy (e.g., it loses ~ 1 point on `cifar100|resnet34`). On `fashion|effb1` it is the fastest algorithm in terms of train loss. On the other hand, it almost never reduces the amount of backtracks below 100 per epoch.
- The step sizes yielded by both Grippo’s adaptations are often growing faster than those of zhang, especially in the initial phase of the optimization procedure. On the other extreme, the monotone line search is too strict and yields step sizes that are very small in comparison to those of zhang. In fact, monotone is achieving very poor results both in terms of train loss and test accuracy.
- `cross_batch_grippo` is never as fast as `single_batch_grippo` in terms of train loss and it loses ~ 5 points of accuracy on `cifar100|resnet34` and `cifar100|densenet121` w.r.t. zhang. In accordance with the conjecture above, `cross_batch_grippo` does not converge on `mnist|mlp`.

In conclusion, zhang (PoNoS) is the best-performing line search technique among those compared in Figure 12. In terms of step size, zhang provides the right middle way between the very permissive Grippo’s conditions and the very strict monotone one. Moreover, even if zhang and `single_batch_grippo` behave similarly, the second is computationally more expensive and it is never able to reduce the backtracks to (almost) always zero.

E.3 Zoom in on the Amount of Backtracks

In this subsection, we zoom in on the amount of backtracks employed by PoNoS and PoNoS_reset0. Instead of showing the cumulative number of backtracks in each epoch (as in the fourth column of Figure 6), Figure 13 reports the amount of backtracks in each iteration. To help visualizing the whole optimization procedure, we average the number of backtracks over 10 consecutive iterations. Respectively on the leftmost and rightmost column of Figure 13 we report the first 20000 iterations and 100 iterations (out of 78200-114600). From these columns we can observe:

- PoNoS_reset0 employs a stable amount of backtracks across iterations.
- PoNoS reduces the number of backtracks to 1 on average already after the first iteration. Afterwards, this value is first stable for the first 1000-10000 iterations (5-25 epochs) and it then reaches a median of 0 after a transition phase.

In the second column of Figure 13, we report the average difference between two consecutive amount of backtracks in the first 20000 iterations. In particular, this value is higher in the initial phase, while (almost) always 0 in a later stage. Focusing on PoNoS_reset0 this difference is almost always below 1. Regarding the newly proposed resetting technique (14), we can conclude that the value l_{k-1} is a good estimate for l_k .

E.4 Study on the Choice of η^{\max}

In this subsection, we report an ablation study on η^{\max} for PoNoS, SLS and SPS. In Figure 14, we compare

- SPS|10: SPS with $\eta^{\max} = 10$. This setting corresponds to SPS.
- SPS|100: SPS with $\eta^{\max} = 100$.
- SLS|10: SLS with $\eta^{\max} = 10$. This setting corresponds to SLS.
- SLS|100: SLS with $\eta^{\max} = 100$.
- PoNoS|10: PoNoS_reset0 with $\eta^{\max} = 10$. This setting corresponds to PoNoS_reset0.
- PoNoS|100: PoNoS_reset0 with $\eta^{\max} = 100$.

We report PoNoS_reset0 (without (14)) instead of PoNoS because we want to observe the difference in the amount of backtracks. To directly observe the effect of changing η^{\max} , we report the average initial step size within each epoch in the third column of Figure 14. From Figure 14 we can observe:

- The value of $\eta^{\max} = 100$ is never reached by the step sizes of the three algorithms. The step size of PoNoS100, SLS100 and SPS100 can be considered unbounded.
- The three algorithms are robust to the choice of η^{\max} . In fact, the train loss and test accuracy of PoNoS100, SLS100 and SPS100 are similar to those of PoNoS10, SLS10 and SPS10.
- In terms of train loss, there are some small differences on `cifar100|resnet34`, `cifar100|densenet121` and `fashion|effb1`. On these problems, PoNoS100, SLS100 and SPS100 are sometimes slower during the intermediate phase of the optimization. However, the three unbounded algorithms are able to catch up towards the end.
- In terms of test accuracy, both SLS100 and SPS100 lose more than 2 points on `cifar100|densenet121` w.r.t. SLS10 and SPS10, while PoNoS100 and SLS100 lose more than 2 points on `cifar100|densenet121`.
- PoNoS100 performs overall better than SLS100 and SPS100.
- The amount backtracks of PoNoS100 is sometimes remarkably larger than for PoNoS10. However, the use of (14) would reduce this number to (almost) always zero.

E.5 Study on the Choice of c_p : Doubling the Legacy Value

In this subsection, we report an ablation study on c_p in (11) for PoNoS and SPS. PoNoS utilize the Polyak step size as an initial guess for the line search method and not as a direct learning rate for SGD as in SPS [Loizou et al., 2021]. We suggest doubling the value employed in Loizou et al. [2021] by employing $c_p = 0.1$ in (11) instead of the default value of $c_p = 0.2$. Given the fact that $\delta = 0.5$, the line search will half the step size when needed, achieving only in this case the same effect of reducing c_p back to $c_p = 0.2$. In Figure 15 we compare

- SPS10.1: SPS with $c_p = 0.1$.
- SPS10.2: SPS with $c_p = 0.2$. This setting corresponds to SPS.
- PoNoS10.1: SLS with $c_p = 0.1$. This setting corresponds to PoNoS.
- PoNoS10.2: SLS with $c_p = 0.2$.

From Figure 15 we can observe that the differences between $c_p = 0.1$ and $c_p = 0.2$ are not remarkable. However, PoNoS10.1 always achieves slightly better performance than PoNoS10.2 both in terms of train loss and test accuracy. On the other hand, the test accuracy of SPS10.1 is not always as high as that achieved by SPS10.2. To conclude, we can observe from the third column of Figure 15 that the step size of PoNoS10.1 is not always larger than that of PoNoS10.2. In fact, this does not happen in the initial phase of the optimization, but in the intermediate phase and only on some problems. Given the improved performance of PoNoS10.1 over PoNoS10.2, one could argue that the line search finds the regions in which a larger step is beneficial.

E.6 Profiling PoNoS

In this subsection, we profile a single mini-batch iteration of PoNoS. More precisely, in Figure 16 we report the time (s) employed by the different operations required to perform an iteration of PoNoS. Averaging along the epoch (over $\frac{M}{b}$ values), in Figure 16 we compare

- 1st_fwd: average time employed to perform the first forward pass;
- 2nd_fwd: average time employed to perform the second forward pass;
- extra_fwd: average time employed to perform all the extra forward passes beyond the second. Notice that the total amount of extra forward passes could be more or less than $\frac{M}{b}$. Despite the actual amount of extra forward passes, we still divide the sum by $\frac{M}{b}$;
- backward: average time employed to perform the backward pass;
- batch_load: average time employed to load a mini-batch of instances into the GPU memory;

From Figure 16, we can observe the following.

- 1st_fwd and 2nd_fwd employ roughly the same time. 2nd_fwd is always slightly faster than 1st_fwd, however, the difference is not substantial.
- A backward pass employs roughly twice the time of a forward pass.
- The time employed to load the mini-batch in the GPU memory is negligible on some networks (`cifar10|densenet121`, `cifar100|densenet121` and `fashion|effb1`). On the other networks, this time is between one-half and 4 times that of a forward pass.
- As previously shown in Figure 13, PoNoS transitions from a phase in which it employs 1 backtrack to 0 (on median). In Figure 16, this same behavior can be also observed in the time employed by all the forward passes beyond the second.

To conclude, the time employed by a single forward pass may reach up to one-third of the computation required for SGD (i.e., `batch_load + 1st_fwd + backward`). Following these calculations and referring to the two phases of Figure 7 and Figure 16, one iteration of PoNoS only costs $\frac{5}{3}$ that of SGD in the first phase and $\frac{4}{3}$ in the second.

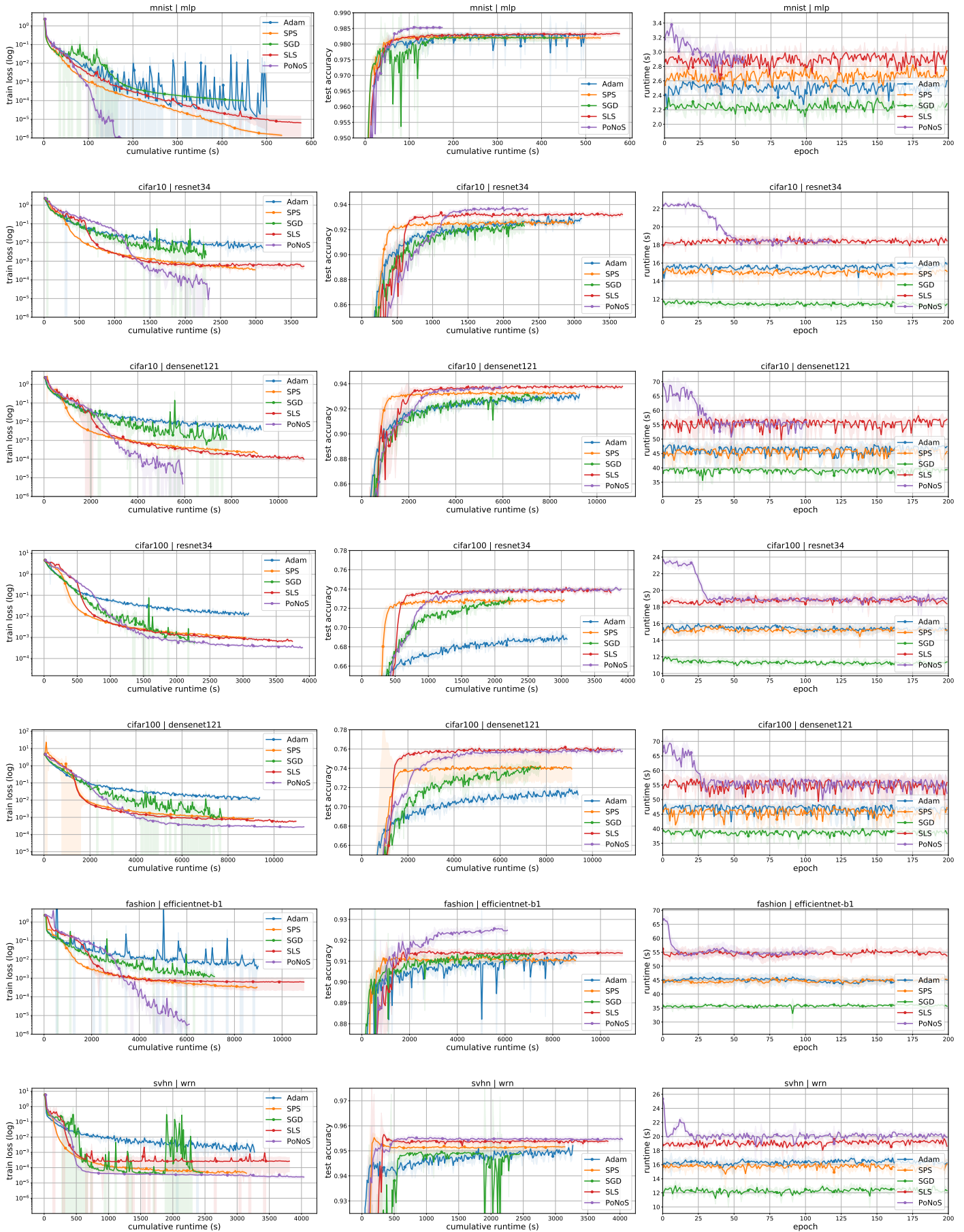


Figure 7: Time comparison (s) between the proposed method (PoNoS) and the-state-of-the-art. Each row focus on a dataset/model combination. First column: train loss vs cumulative runtime. Second column: test accuracy vs cumulative runtime. Third column: per-epoch runtime.

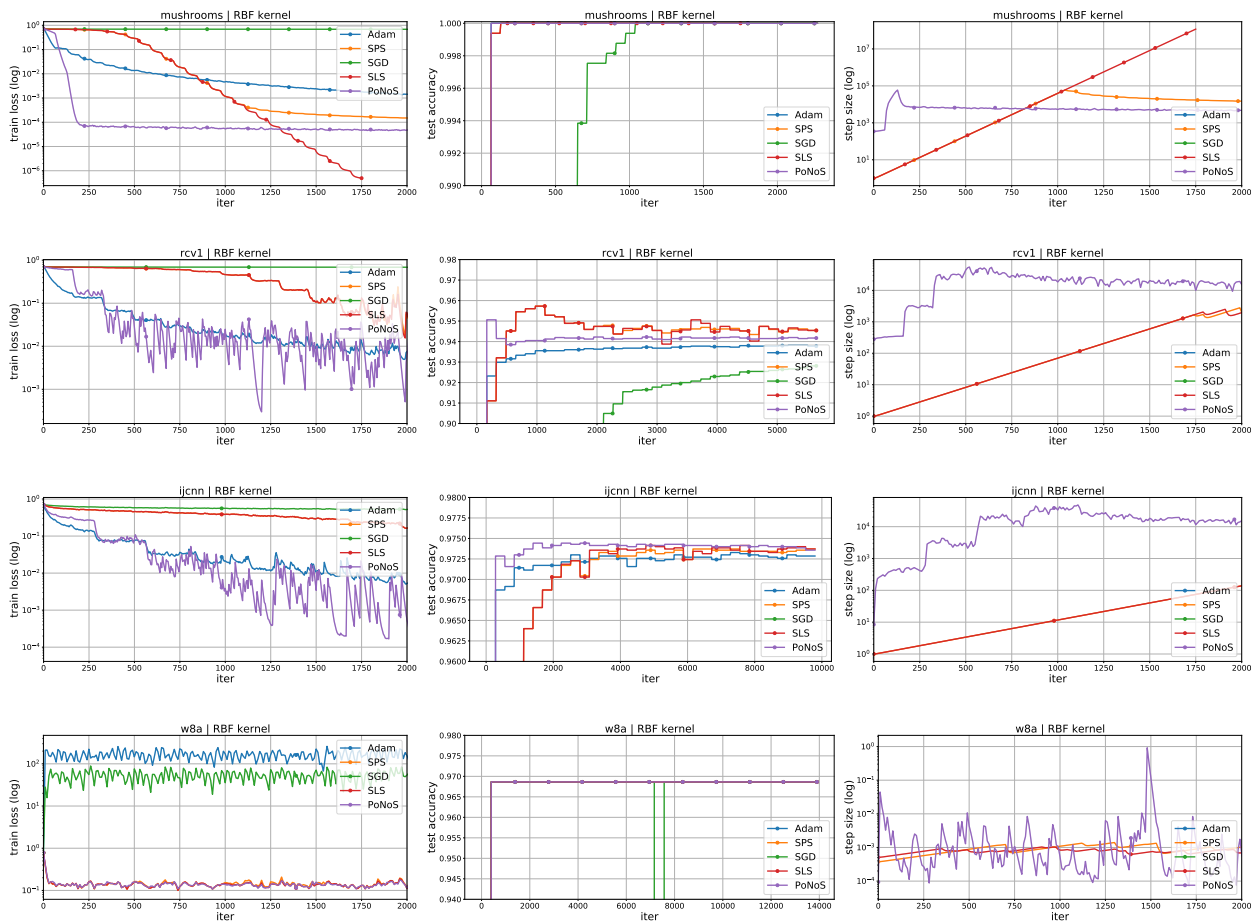


Figure 8: Comparison between the proposed method (PoNoS) and the state-of-the-art on convex kernel models for binary classification. Each row focus on a different dataset. First column: exponentially averaged train loss. Second column: test accuracy. Third column: exponentially averaged step size.

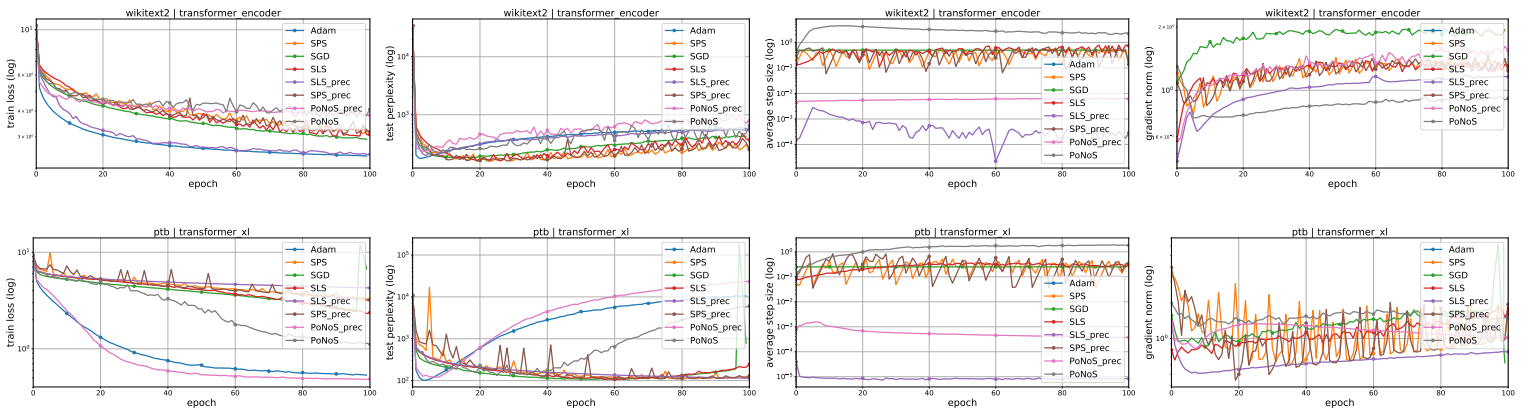


Figure 9: Comparison between the proposed method (PoNoS) and the state-of-the-art on the training of transformers for language modeling tasks. Each row focus on a dataset/model combination. First column: train loss. Second column: train perplexity. Third column: average step size. Fourth column: average gradient norm.

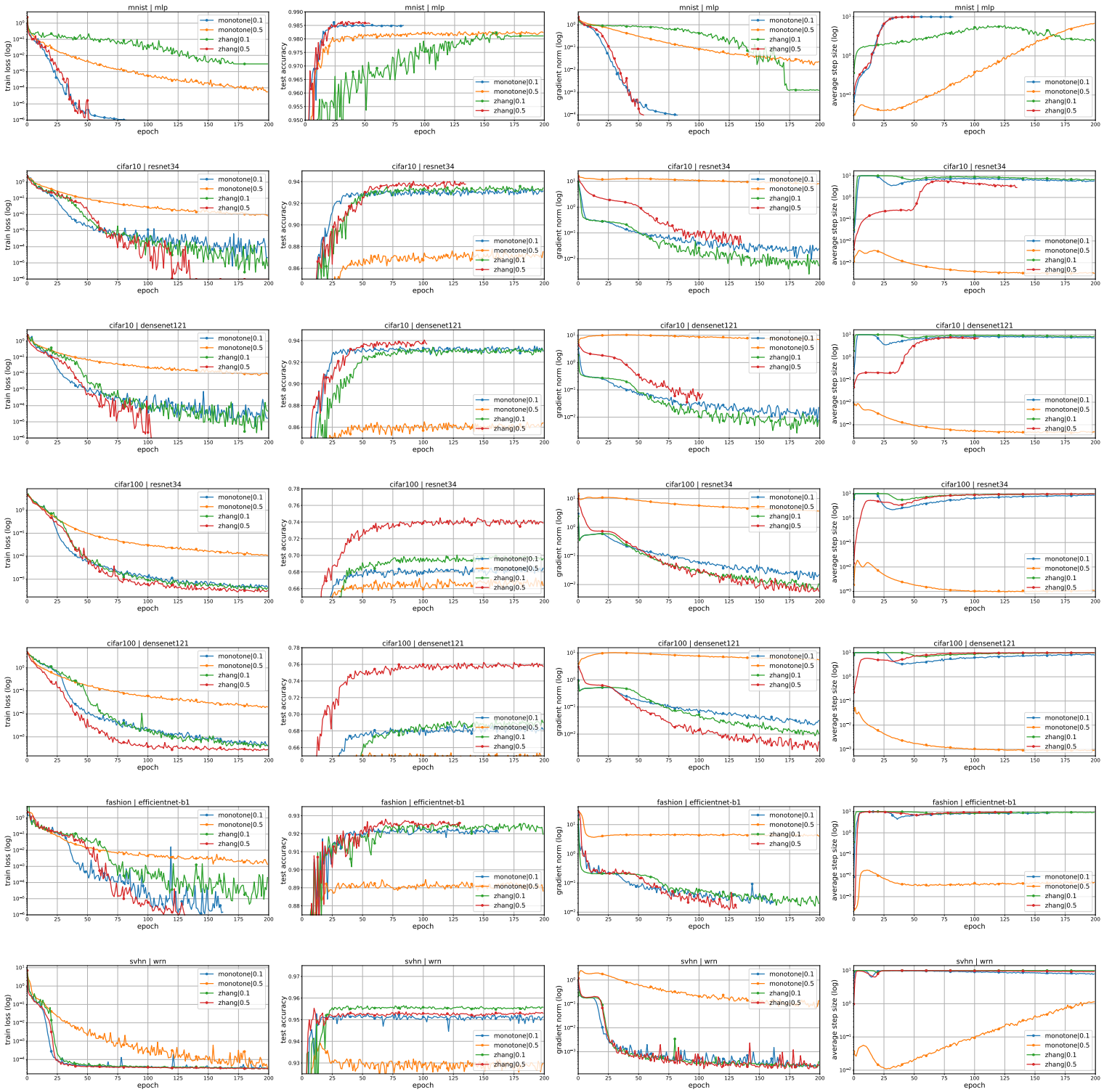


Figure 10: Comparison between the use of the constant $c = 0.1$ and $c = 0.5$ on both monotone and nonmonotone algorithms. Each row focus on a dataset/model combination. First column: train loss. Second column: test accuracy. Third column: average step size of the epoch. Fourth column: average gradient norm of the epoch.

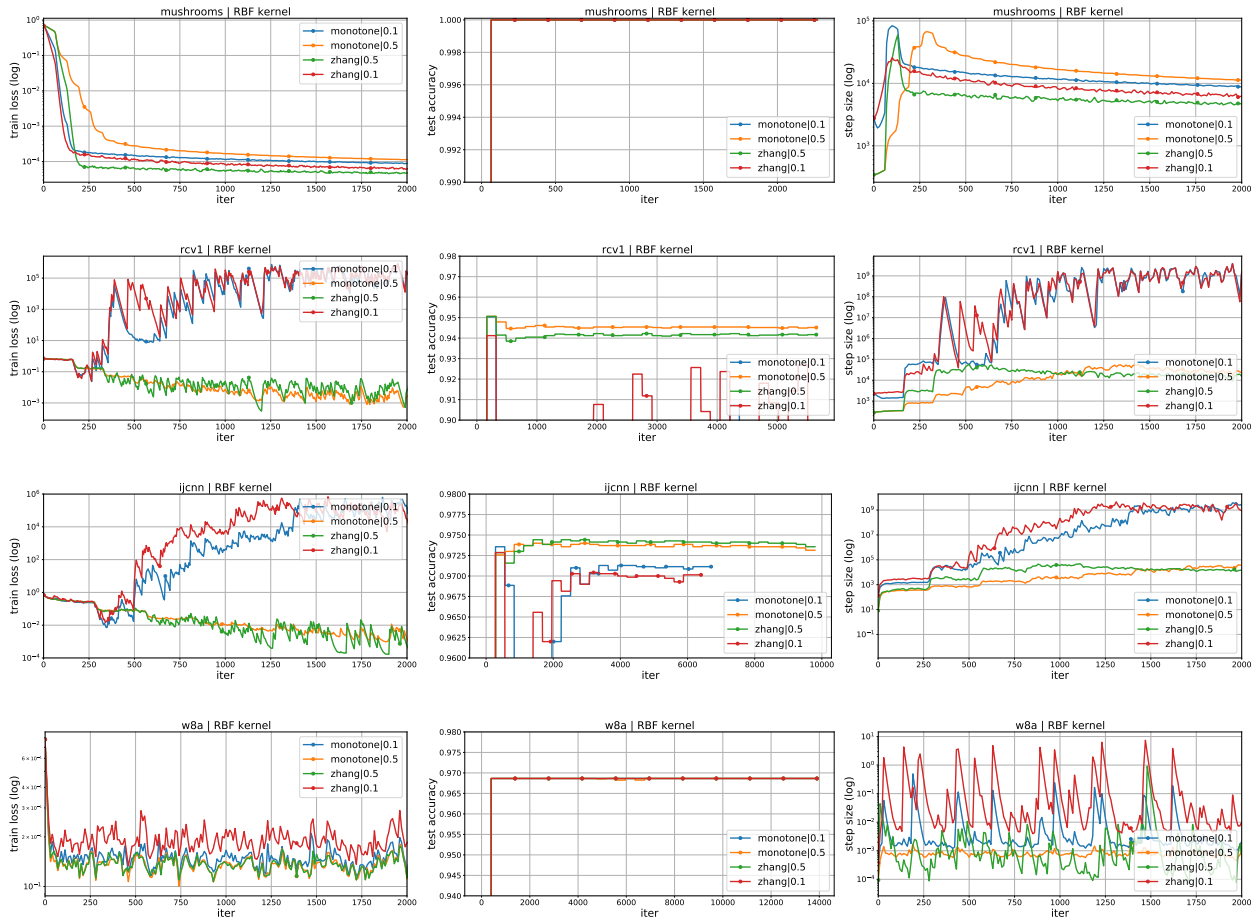


Figure 11: Comparison between the use of the constant $c = 0.1$ and $c = 0.5$ on both monotone and nonmonotone algorithms on convex binary classification problems. Each row focus on a different dataset. First column: exponentially averaged train loss. Second column: test accuracy. Third column: exponentially averaged step size.

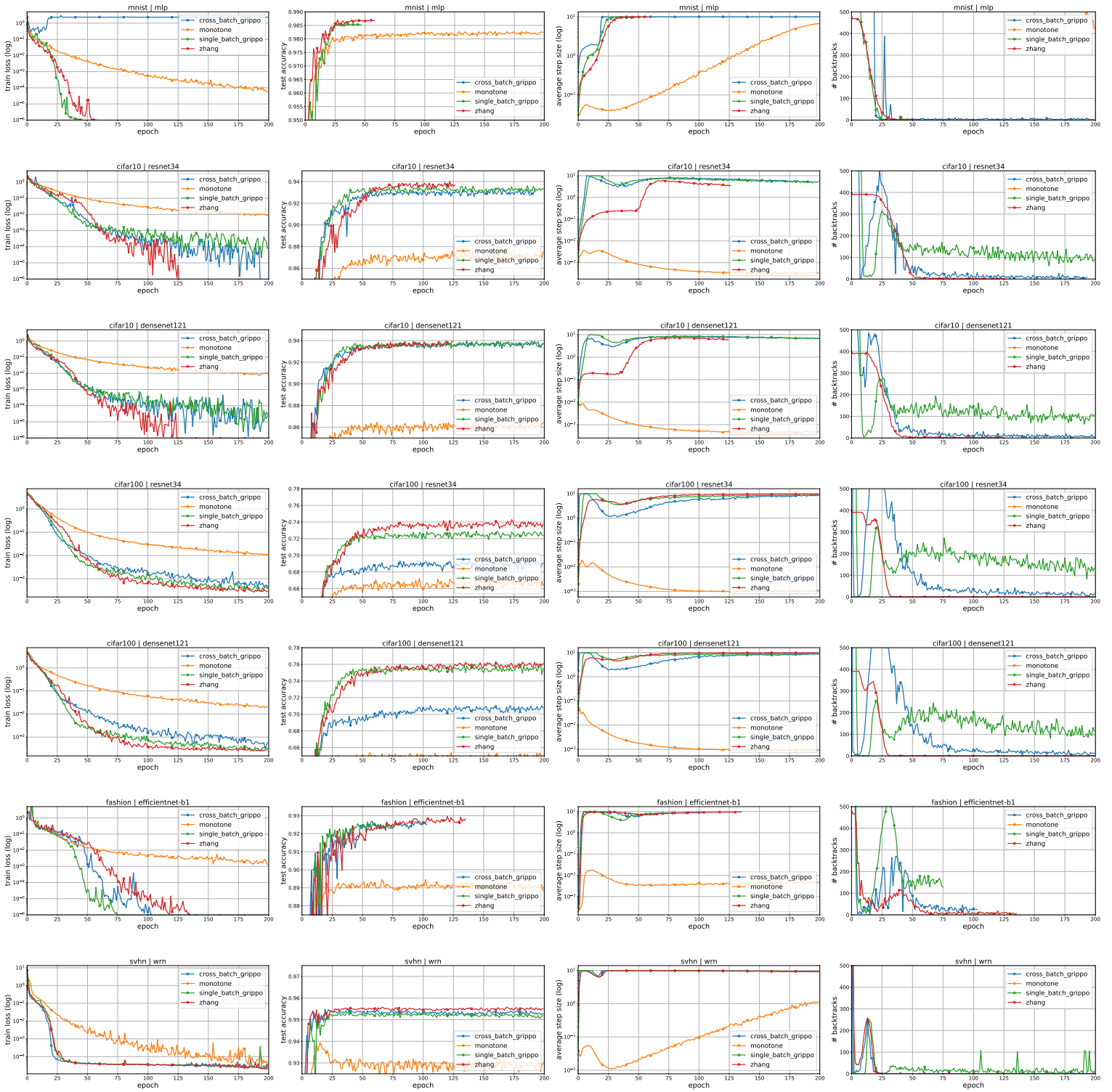


Figure 12: Comparison between different monotone and nonmonotone line search conditions. Each row focus on a dataset/model combination. First column: train loss. Second column: test accuracy. Third column: average step size of the epoch. Fourth column: cumulative number of backtracks in the epoch.

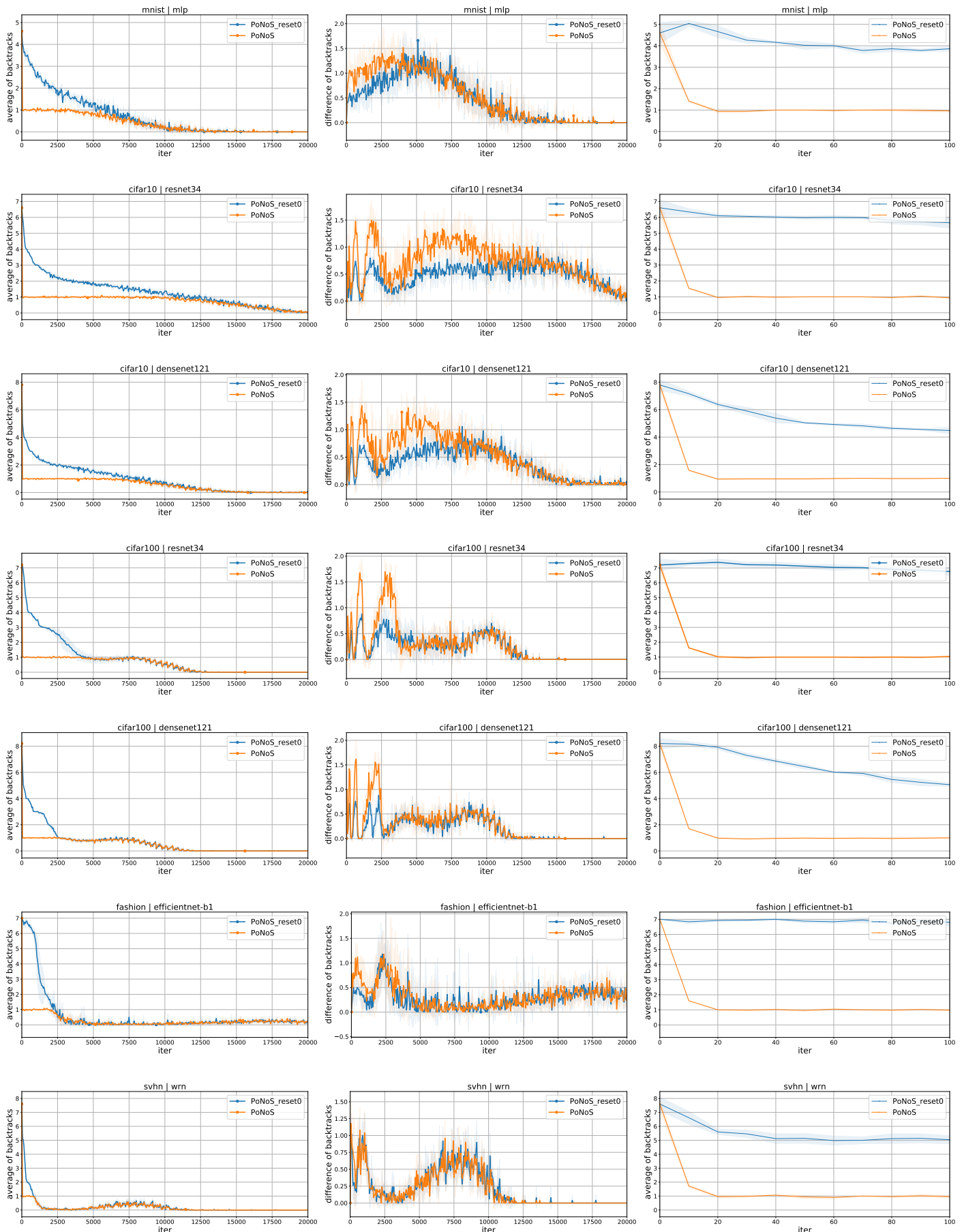


Figure 13: Comparison on the number of backtracks between the proposed method with (PoNoS) or without the new resetting technique (PoNoS_reset0). Each row focus on a dataset+model combination. First column: average number of backtracks in the first 200000 iterations. Second column: average difference between two consecutive amount of backtracks in the first 200000 iterations. Third column: average number of backtracks in the first 1000 iterations.

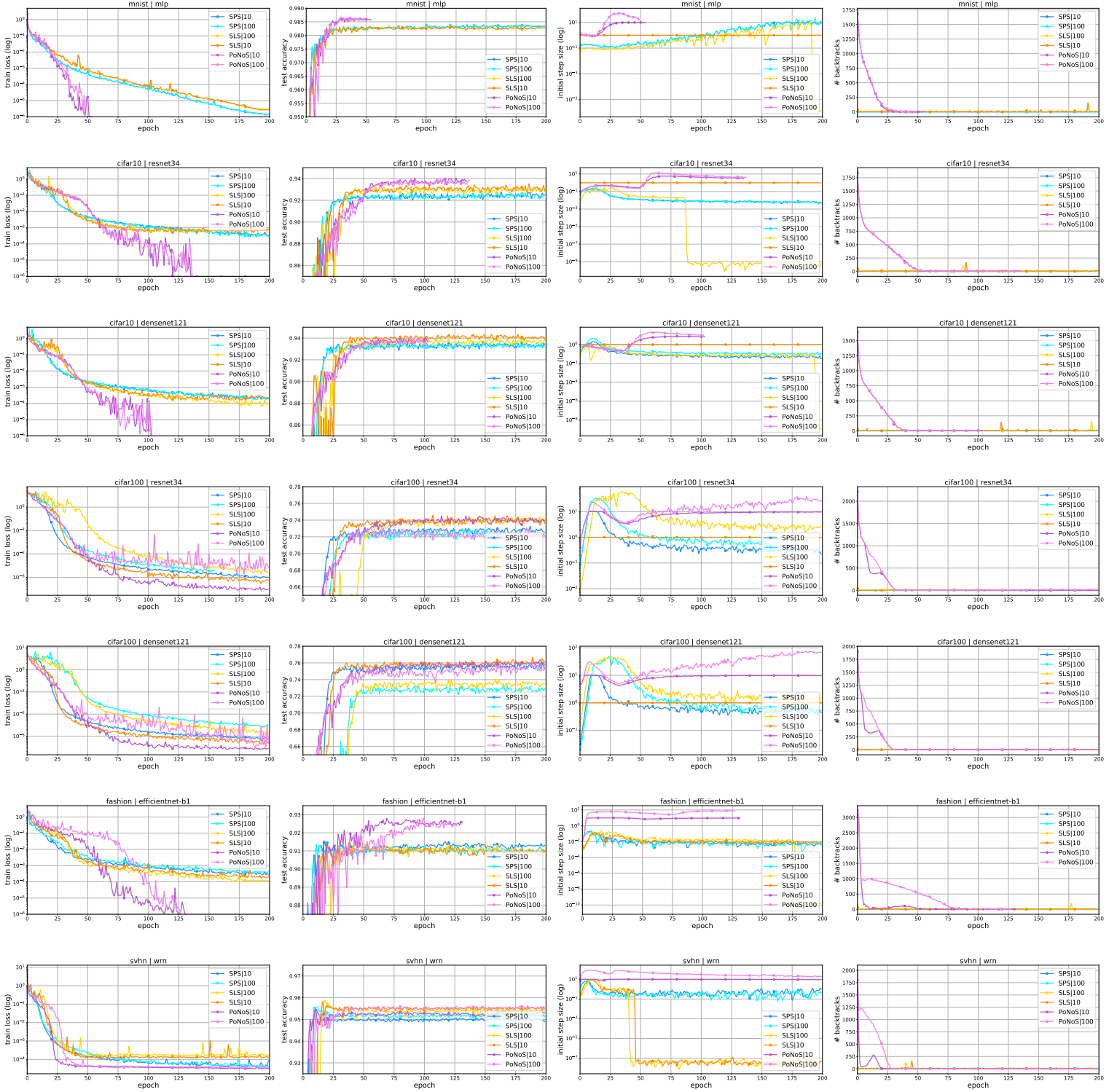


Figure 14: Comparison between the use of the constant $\eta^{\max} = 10$ and $\eta^{\max} = 100$ on SPS, SLS and PoNoS. Each row focus on a dataset/model combination. First column: train loss. Second column: test accuracy. Third column: average initial step size of the epoch. Fourth column: cumulative number of backtracks in the epoch.

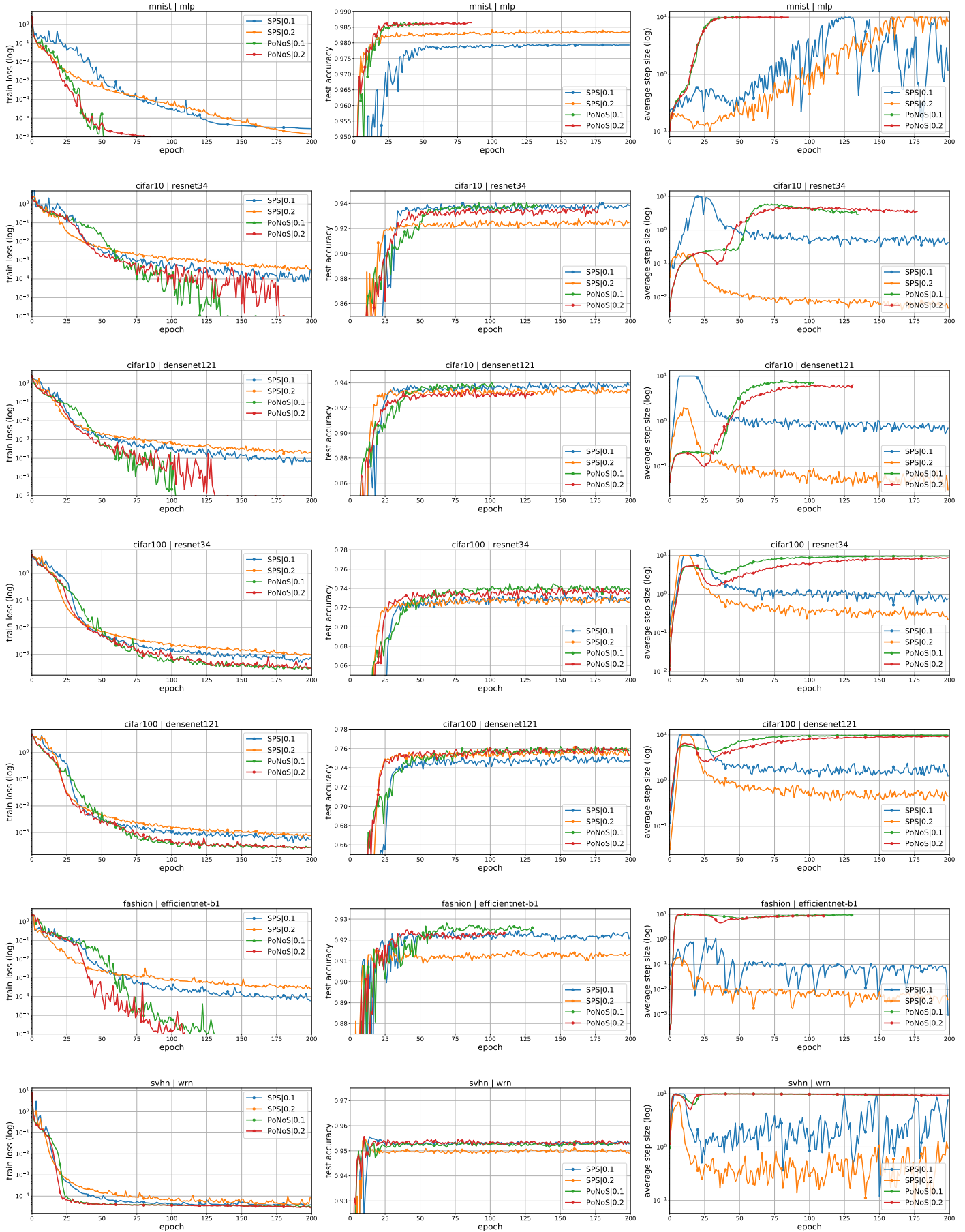


Figure 15: Comparison between the use of the constant $c_p = 0.1$ and $c_p = 0.2$ on PoNoS and SPS. Each row focus on a dataset/model combination. First column: train loss. Second column: test accuracy. Third column: average step size of the epoch.

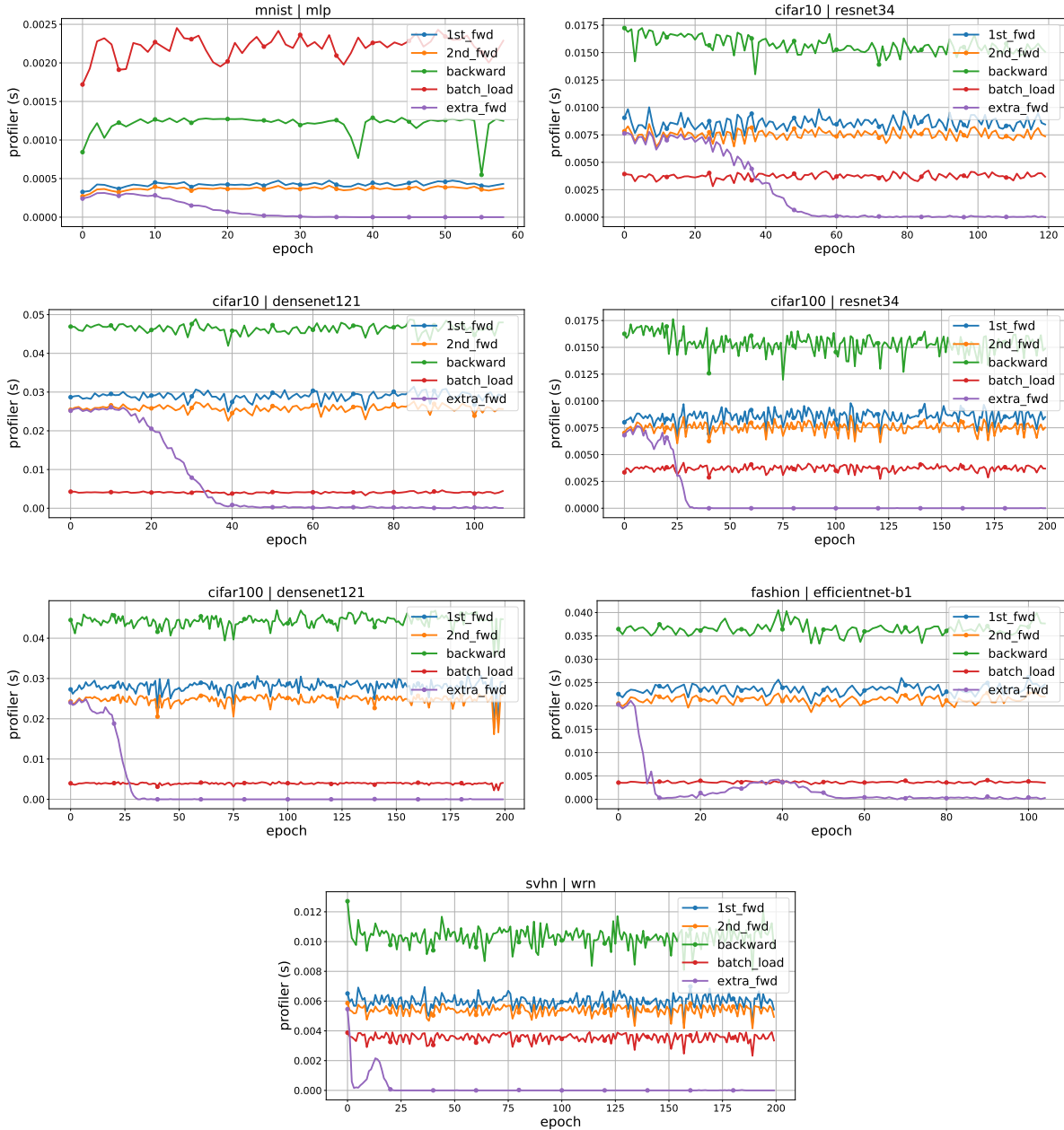


Figure 16: Profiling of a single iteration of PoNoS. We report the time of the 1st and second forward passes, the time of all the extra forward passes beyond the second, the time of the backward pass and the time to load the mini-batch in the GPU.